ISSN Application No. 25023

Indian Journal of Civil and Mechanical Engineering

Volume No. 7

Issue No. 1

January - April 2024

ENRICHED PUBLICATIONS PVT. LTD

S-9, IInd FLOOR, MLU POCKET,
MANISH ABHINAV PLAZA-II, ABOVE FEDERAL BANK,
PLOT NO-5, SECTOR-5, DWARKA, NEW DELHI, INDIA-110075,
PHONE: - + (91)-(11)-47026006

ISSN Application No. 25023

Indian Journal of Civil and Mechanical Engineering

Aims and Scope

Indian Journal of Civil and Mechanical Engineering publishes the original papers within the broad field of civil mechanical engineering which include, but are not limited to, the following: Surveying and Geodesy. Construction Management, Geotechnical Engineering, Highway Engineering, Information Technology, Nuclear Power Engineering, Railroad Engineering, Structural Engineering, Surveying and Geo-Spatial Engineering, Tunnel Engineering, Water Engineering, Coastal and Harbor Engineering, Architecture and Construction Engineering, Environmental Engineering, Materials Engineering, Structural Engineering, Water and Sanitary Engineering, Transportation Engineering.

Theoretical papers, practice-oriented papers including case studies, state-of-the-art reviews are all welcomed and encouraged for the advance of science and technology in civil engineering.

Submission of Paper : Manuscripts are invited from academicians, research students, and scientists for publication consideration. Papers are accepted for editorial consideration through email info@enrichedpublications.com with the understanding that they have not been published, submitted or accepted for publication elsewhere. Please mention journal title in your email.

ISSN Application No. 25023

Indian Journal of Civil and Mechanical Engineering

ISSN Application No. 25023

Indian Journal of Civil and Mechanical Engineering

(Volume No. 7, Issue No. 1, January - April 2024)

Contents

Groundwater Suitability for Irrigation in Pulicat Using GIS

[1]P Abraham Daniel Raj, [1]E Arivoli, [1]M Hemalatha
[1]PG Student, M.E Integrated Water Resources Management
Centre for Water Resources, Anna University, Chennai 600025, Tamil Nadu, India
Email: arivoli.e@gmail.com , hemalathamuruges@gmail.com
Mobile: 9943387788 / 9500291922

A B S T R A C T

India is an agricultural country. About seventy per cent of its people depend on agriculture. Watering is essential for the crops. Rainfall in India is erratic India gets almost all of its rainfall during the rainy season from June to September. But the rainfall is not uniform. Irrigated Agriculture does not depend only on surface water available. It can be sustained by conjunctive use of surface and groundwater available. To find the suitability of ground water in Pulicat, Tamil Nadu, India for irrigation, the present study mainly focused on the physico-chemical analysis of ground water (well and bore water samples).The selected ground water quality parameters for this study are pH, total dissolved solids (TDS), total hardness (TH), calcium (Ca^{2+}) magnesium (Mg^{2+}), sodium (Na^{+}), potassium (K^{+}), carbonate (CO_3^{-}), bicarbonate (HCO_3^{-}). To find the suitability for irrigation, the selected indices for this present study are sodium adsorption ratio (SAR), soluble sodium percentage (SSP), residual sodium bicarbonate (RSBC), permeability index (PI), magnesium adsorption ratio (MAR), and Kelly's ratio (KR).The obtained results were depicted using GIS tool in order to get the continuous value and to suggest the better place for farming. Present study recommends that the top priority has to be given to water quality monitoring. The results have indicated that most of the irrigation water quality indices showed unsatisfactory result which proved that the water is unfit for cultivation. But it is found that some salt tolerant crops can also be grown in the selected study area.

Keywords: Ground water, Irrigation water quality indices, Physico-chemical parameters.

1. Introduction

India is an agricultural country. About seventy per cent of its people depend on agriculture. Watering is essential for the crops. Agriculture is not possible without water. Rainfall in India is erratic India gets almost all of its rainfall during the rainy season from June to September. The rainfall is not uniform. Some parts get heavy rainfall, some parts get moderate rainfall and some parts are left without rainfall. If the rivers get flooded, this damages the life, property and crops. The rainfall also varies from year to year. Thus, it needs to regulate the watering for crops through irrigation. This study mainly focused on finding the suitability of groundwater for irrigation near Pulicat Lake, through the analysis of various irrigation indices are sodium adsorption ratio (SAR), soluble sodium percentage (SSP), residual sodium bicarbonate (RSBC), permeability index (PI), magnesium adsorption ratio (MAR), and Kelly's ratio (KR).

1.1 STUDY AREA

Pulicat Lake is the second largest brackish water lake in India. It situated in the border of Andhra Pradesh and Tamil Nadu. The lagoon's boundary limits range between 13.33° to 13.66° N and 80.23° to 80.25°E, with a dried part of the lagoon extending up to 14.0°N.; with about 84% of the lagoon in Andhra Pradesh and 16% in Tamil Nadu. The lagoon is aligned parallel to the coast line with its western and eastern parts covered with sand ridges. Area of the lake varies with the tide; 450 square kilometers (170 sq mi) in high tide and 250 square kilometeres (97 sq mi) in low tide. Its length is about 60 kilometers (37 mi) with width varying from 0.2 kilometers (0.12 mi) to 17.5 kilometers (10.9 mi). The study area has been divided into three zones and the irrigation water quality and the irrigation water standards are compared for these three zones.

2. MATERIALS AND METHODS

The entire pulicat is divided into 3 areas suitable for irrigation and in total of Twenty Eight samples (well and bore points) were collected randomly in the area and their corresponding latitudes and longitudes were noted using gramin hand held GPS. The water samples were collected in well cleaned plastic bottles without the presence of air bubbles. The sampling locations were randomly selected throughout the study area.

Physico-chemical parameters such as TDS, Electrical Conductivity, Calcium, Magnesium, Sodium, Carbonate, Potassium etc. for these samples were determined by using standard procedures (APHA, 2005). The values of these physico-chemical parameters are used to determine the irrigation water quality indices such as sodium adsorption ratio (SAR), soluble sodium percentage (SSP), residual sodium bicarbonate (RSBC), permeability index (PI), magnesium adsorption ratio (MAR) and kelly's ratio (KR).

Table 1 Details about water sample in area

SAMPLE NO	POSITION		PLACE	TYPE OF SAMPLE
	LAT	LON		
1	N 13°25.31′	E 80°19.47′	AREA 1 (LEFT TO THE BRIDGE)	BORE
2	N 13°25.39′	E 80°19.49′		
3	N 13°25.41′	E 80°19.54′		
4	N 13°25.36′	E 80°19.53′		
5	N 13°25.31′	E 80°19.56′		
6	N 13°25.34′	E 80°19.60′		
7	N 13°25.37′	E 80°19.68′		
8	N 13°25.39′	E 80°19.65′		
9	N 13°25.44′	E 80°19.61′		

Table 1.1 Details about water sample in area 2

SAMPLE NO	POSITION		PLACE	TYPE OF SAMPLE
	LAT	LON		
1	N 13°25.22′	E 80°19.54′	AREA 2 (RIGHT TO THE BRIDGE)	BORE
2	N 13°25.16′	E 80°19.58′		
3	N 13°24.93′	E 80°19.53′		
4	N 13°24.97′	E 80°19.63′		
5	N 13°24.90′	E 80°19.67′		
6	N 13°25′	E 80°19.62′		
7	N 13°25.01′	E 80°19.57′		
8	N 13°25.03′	E 80°19.54′		
9	N 13°25.03′	E 80°19.60′		
10	N 13°25.11′	E 80°19.59′		

Table 1.2 Details about water sample in area 3

SAMPLE NO	POSITION		PLACE	TYPE OF SAMPLE
	LAT	LON		
1	N 13°24.43′	E 80°19.13′	AREA3 (SATTANKUPPAM)	OPEN WELL
2	N 13°24.40′	E 80°19.17′		OPEN WELL
3	N 13°24.42′	E 80°19.21′		BORE
4	N 13°24.45′	E 80°19.25′		BORE
5	N 13°24.50′	E 80°19.24′		BORE
6	N 13°24.51′	E 80°19.24′		BORE
7	N 13°24.51′	E 80°19.26′		OPEN WELL
8	N 13°24.50′	E 80°19.20′		BORE
9	N 13°24.55′	E 80°19.18′		BORE

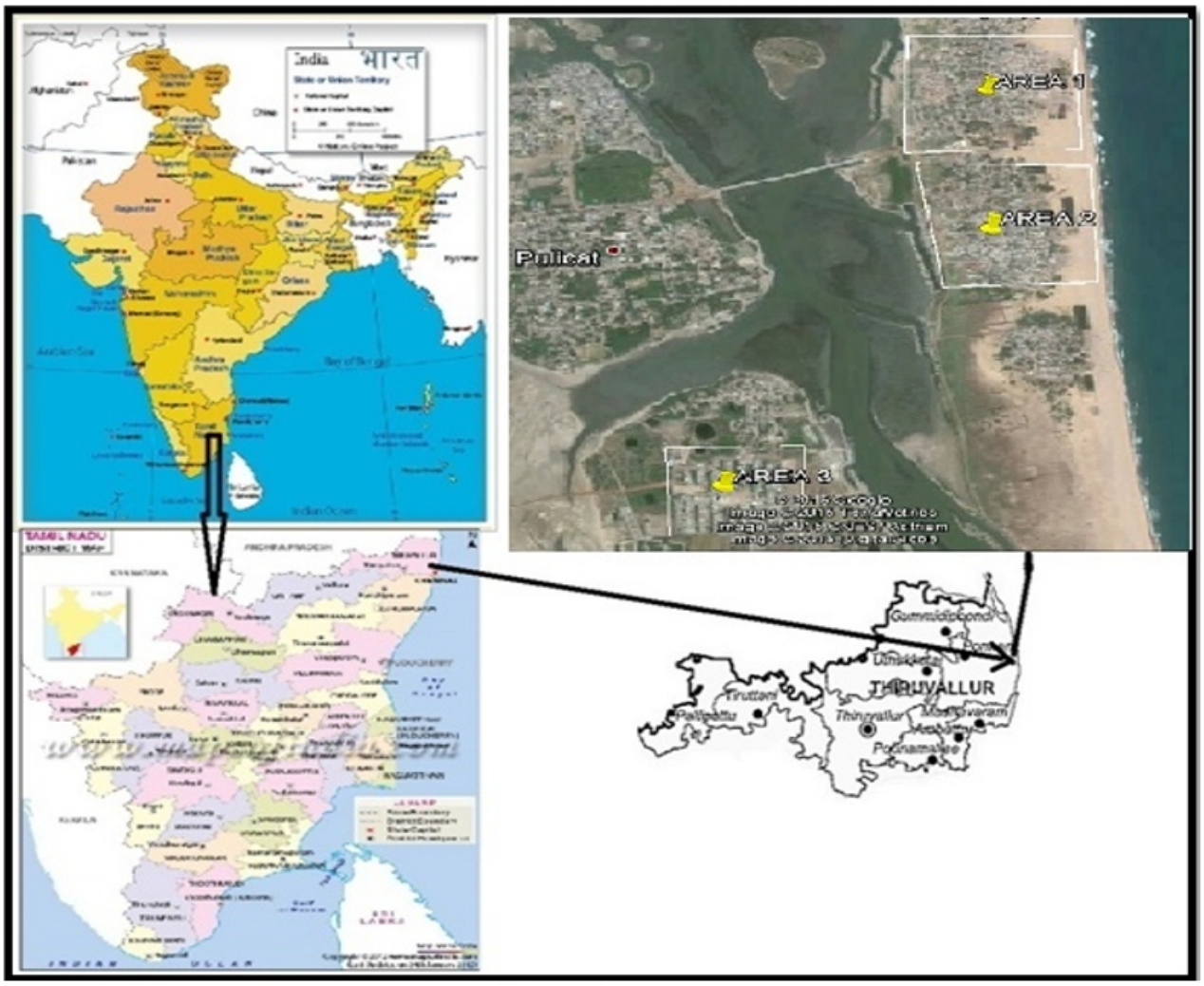

Fig 1 Study Area

3. RESULTS AND DISCUSSIONS

Geochemical properties and principles that govern the behaviour of dissolved chemical constituents in groundwater are referred to as hydro geochemistry. The dissolved constituent exists as ions, molecules or solid particles, these constituent not only undergo chemical and physical reactions but also redistribution takes place among the various ionic species this can also take place between the liquid and solid phases.

The physical and chemical composition of groundwater is directly related to the solid product of rock weathering and changes with respect to time and space surrounding it. Therefore, the variation on the concentration levels of the different physico-chemical constituents dissolved in water determines its utility for domestic, industrial and agricultural purposes.

In this study, the results of the analysed physico-chemical parameters were correlated with those of the various irrigation indices.

Table 2 The Experimental Results of Physico-Chemical Properties and the Values of Various Irrigation Water Quality Indices

PARAMETERS/AREA	*AREA 1(10 SAMPLES)*	*AREA 2(10 SAMPLES)*	*AREA 3(9 SAMPLES)*
pH	*7.16*	*7.42*	*7.69*
EC µs/cm	*984.44*	*2312*	*1940*
Ca mg/l	46.84	79.65	48.312
Mg mg/l	25.94	53.02	52.44
Na mg/l	98.35	303.14	246.08
K mg/l	8.42	20.41	7.84
TDS mg/l	518.67	1303.5	1051.5
RSC	0.11	0.72	1.71
SAR	2.68	3.9	6.7
SSP	49.40	62	62.17
MAR	45.51	52.61	66.97
KR	0.93	1.57	1.62
PI	2.82	1.62	1.87

The Table 2 shows the experimental results of physico chemical properties and the values of various irrigation water quality indices.

3.1 ELECTRICAL COUNDUCTIVITY

Table 3 The Standard Values for EC

Salinity Hazard Class	EC, (µs/cm)	Remark on quality
C1	100-250	Excellent
C2	250-750	Good
C3	750-2250	poor
C4	>2250	Unsuitable

The electrical conductivity of the water samples collected ranges between 985 and 2312, (Table 2) only very few water samples collected comes under good and excellent classes and most of the water sample have salinity hazard leading to its unsuitability for irrigation purpose.

3.2 SODIUM ADSORPTION RATIO

The sodium adsorption ratio gives a clear idea about the adsorption of sodium by soil. It is the proportion of sodium to calcium and magnesium, which affects the availability of the water to the crop.

The Sodium Adsorption Ratio (SAR) can be calculated by the following equation given by Richards (1954) as:

$$SAR = \frac{Na}{\sqrt{(Ca+Mg)/2}}$$

Where all the ions are expressed in meq/L.

The SAR value can be used to determine the sodium hazard classes of different water samples from the table below.

Table 4 The Standard Values for SAR

Sodium hazard class	SAR	Remark on quality
S1	<10	Excellent
S2	10-18	Good
S3	18-26	Doubtful
S4	>26	Unsuitable

The SAR values of all the samples are below 10 (TABLE 2) which show that the irrigation water quality of all samples of the study area with respect to SAR is excellent (TABLE4).

3.3 SOLUBLE SODIUM PERCENTAGE (SSP)

Sodium percent is an important factor for studying sodium hazard. It is also used for adjudging the quality of water for agricultural purposes. High percentage sodium water for irrigation purpose may stunt the plant growth and reduces soil permeability (Joshi et al., 2009).The soluble sodium percentage values of shallow groundwater in the study area ranges between 49 and 62.17(TABLE 2) indicating very high alkali hazards. Thus the water has to be treated before it is used for the purpose of irrigation otherwise there is a serious possibility of crop failure which may lead to huge economic loss for the farmers.

The Soluble Sodium Percentage (SSP) can be calculated by the following equation (Todd, 1995):

$$SSP = \frac{(Na+K)\times 100}{Ca+Mg+Na+K}$$

where, all the ions are expressed in meq/L.

3.4 RESIDUAL SODIUM BICARBONATE (RSBC)

The concentration of bicarbonate and carbonate influences the suitability of water for irrigation purpose. The water with high RSBC has high pH. Therefore, land irrigated with such water becomes infertile owing to deposition of sodium carbonate (Eaton, 1950). The residual sodium bicarbonate values of water samples from the study area ranges from9.6 in area 1 to 19.02 in area 2 while area3 has a RSBC value of 16.95meq/l. Since the values are greater than 3meq/l the water has to undergo treatment before using it for irrigation.

The Residual Sodium Bicarbonate (RSBC) can be calculated according to Gupta and Gupta (1987):

$RSBC = HCO_3 \times Ca$

where, RSBC and the concentration of the constituents are expressed in meq/L.

3.5 MAGNESIUM ADSORPTION RATIO (MAR)

Magnesium content of water is considered as one of the most important qualitative criteria in determining the quality of water for irrigation. Generally, calcium and magnesium maintain a state of equilibrium in most waters. More magnesium in water will adversely affect crop yields as the soils become more saline (Joshi et al., 2009). The values of the magnesium adsorption ratio of shallow groundwater in present study varies from 46 to 67 (TABLE 2) indicating that they are above the acceptable limit of 50% (Ayers and Westcot, 1985). The most of the water samples in the study area are prone to magnesium hazard.

The Magnesium Adsorption Ratio (MAR) can be calculated using the following equation (Raghunath, 1987):

$$MAR=\frac{Mg\times 100}{Ca+Mg}$$

Where, all the ionic constituents are expressed in meq/L.

3.6 TOTAL DISSOLVED SOLIDS (TDS)

Salts of calcium, magnesium, sodium, potassium present in the irrigation water may prove to be injurious to plants. When present in excessive quantities, they reduce the osmotic activities of the plants and may prevent adequate aeration. The TDS value of the study area ranges from 519 to 1304 mg/L (TABLE 2)They are generally higher than 450 mg/L and can be classified as unsuitable as irrigation water according to Robinove et al. (1958). The Total Dissolved Solids (TDS) was calculated employing the following equation (Richards 1954):

$$TDS = 0.64 \times EC \times 10^{6}$$

where, Electrical Conductivity (EC) and TDS are expressed in μ-mhos/cm and mg/L, respectively.

3.7 PERMEABILITY INDEX (PI)

The soil permeability is affected by the long-term use of irrigated water and the influencing constituents are the total dissolved solids, sodium bicarbonate and the soil type. In the present study, the permeability index values range between 2.1 to 4.8. (TABLE 2)The water samples can be categorized as good irrigation water (Doneen, 1964). The Permeability Index (PI) was calculated according to Doneen (1964) employing the following equation:

$$PI = \frac{Na + \sqrt{(HCO3 \times 100)}}{Ca + Mg + Na}$$

where, all the ions are expressed in meq/L.

3.8 KELLYS RATIO (KR) The kellys Ratio (KR) values of the study area ranged between 0.93 and 1.62 .These indicate that Most of the KR for the shallow groundwater samples does not fall within the permissible limit of 1.0 and are considered unsuitable for irrigation purposes. The Kelly's Ratio can be calculated employing the Following equation (Kelly, 1963) as

$$KR = \frac{Na}{Ca + Mg}$$

where, all the ionic constituents are expressed in meq/L.

4. SPATIAL DISTIBUTION OF PARAMETERS USING GIS

4.1 pH

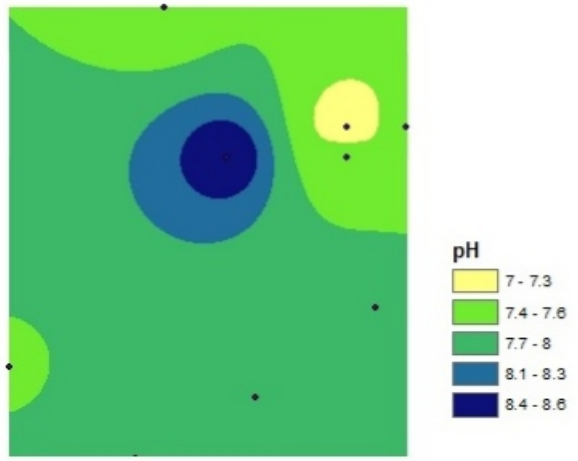

Fig 2 pH distribution in study area 1

4.2 ELECTRICAL CONDUCTIVITY

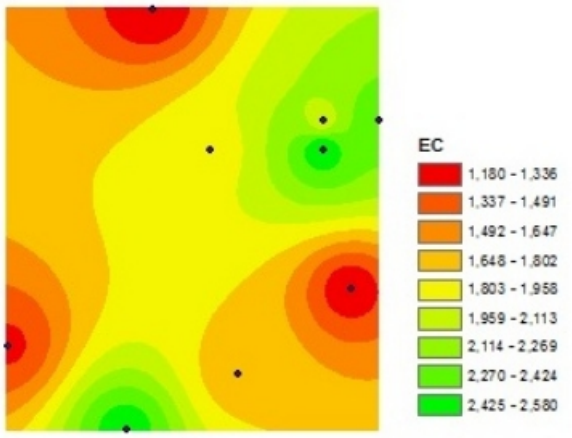

Fig 3 Electical Conductivity distribution in study area 1

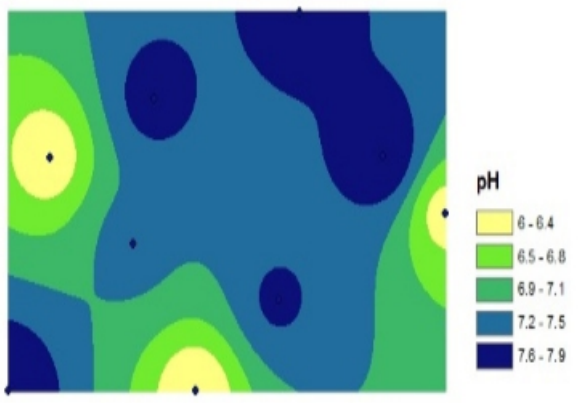

Fig 2 a pH distribution in study area 2

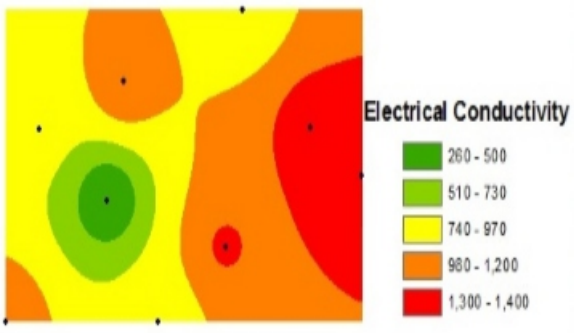

Fig 3 a Electical Conductivity distribution in study area 2

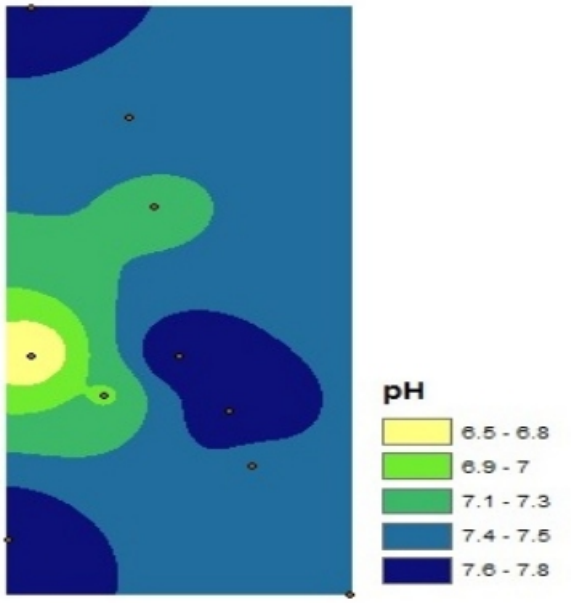

Fig 2 b pH distribution in study area 3

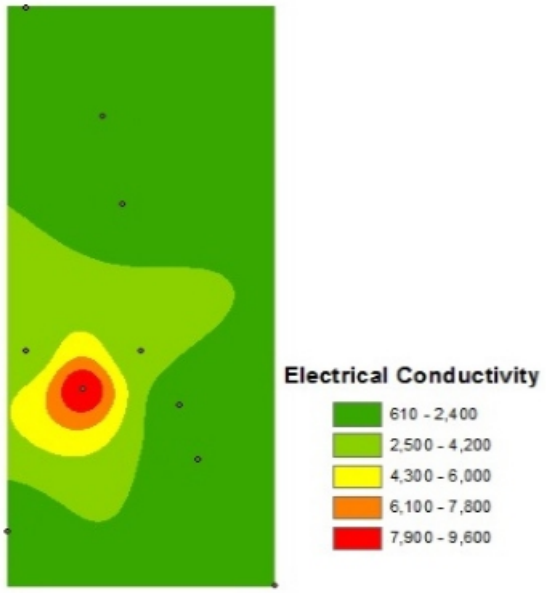

Fig 3 b Electical Conductivity distribution in study area 3

4.3 SODIUM ADSORPTION RATIO (SAR)

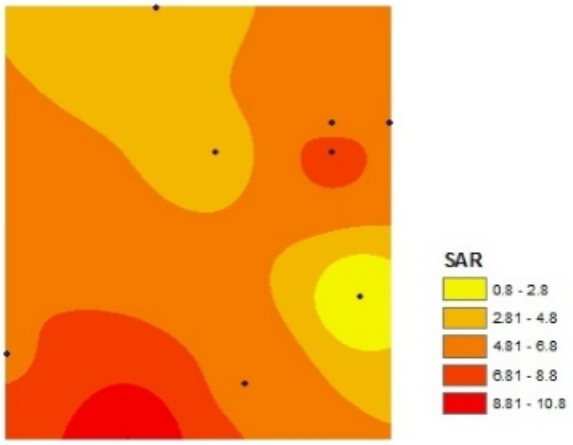

Fig 4 Sodium Adsorption Ratio (SAR) distribution in study area 1

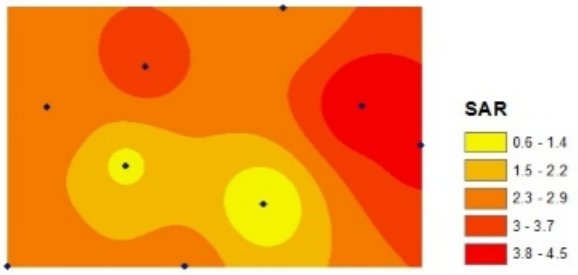

Fig 4 a Sodium Adsorption Ratio (SAR) distribution in study area 2

4.4 TOTAL HARDNESS

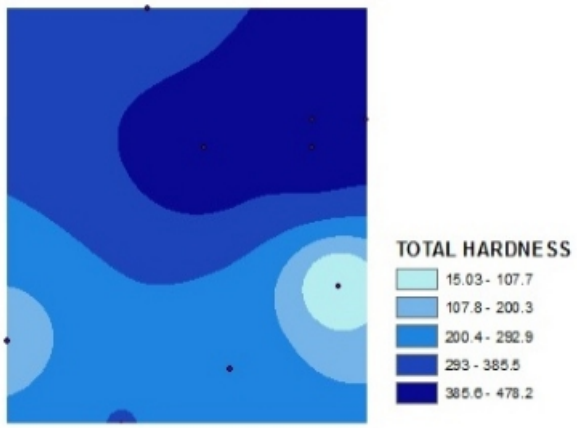

Fig 5 Total Hardness distribution in study area 1

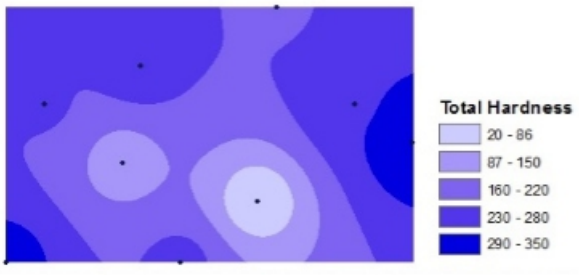

Fig 5 a Total Hardness distribution in study area 2

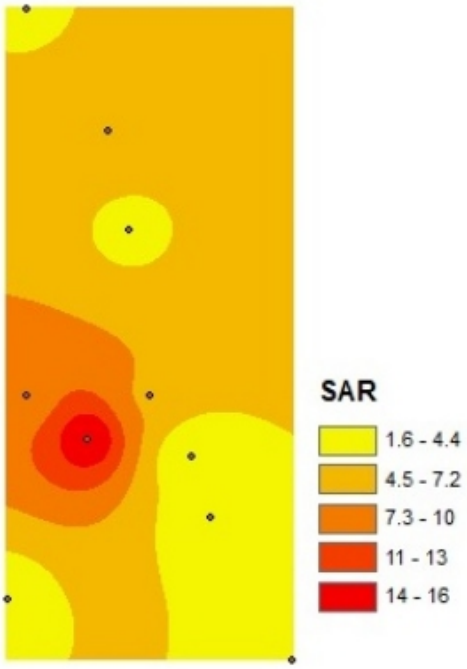

Fig 4 b Sodium Adsorption Ratio (SAR) distribution in study area 3

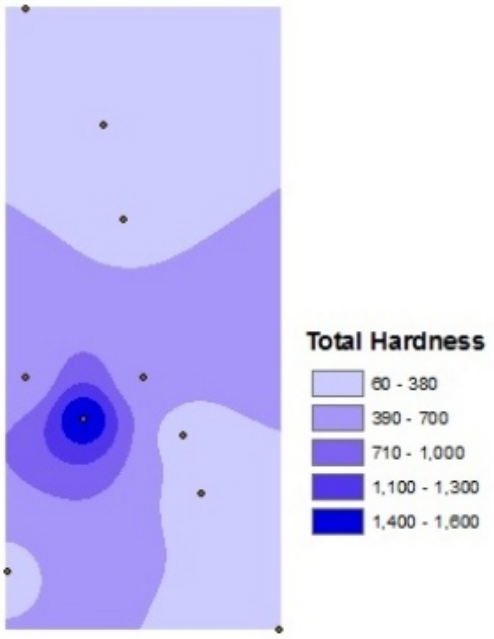

Fig 5 b Total Hardness distribution in study area 3

5. CONCLUSION

Thus, the present study has proved experimentally that most of the irrigation water quality indices determined a show unsatisfactory result which proves that the water is unfit for cultivation.

6. RECOMMENDATIONS

It can be found that the irrigation water quality indices are not to the extreme poor, thus some salt tolerant crops can be grown in that area so as to meet the economic support not only from fisheries but also from agricultural sector. Conjunctive use of ground water will sustain agriculture in coastal areas. High salt tolerant crops like rice, tobacco can be grown in the area.2 with EC ranging between 2to 2.5 ds/m. Also some other crops like foxtail millet, musk melon, pigeon pea, pumpkin, watermelon etc, have the potential to be grown in area 1 and area 2 with less than 2ds/m electrical conductivity. Intensive agriculture is not both socially and politically viable, however few vegetable and fruit crops can be grown commercially or in a small scale as kitchen gardening which sustains the people income.

7. REFERENCES

1. *APHA, Standard Methods for the Examination of Water and Wastewater. APHA-AWWA-WPCF 1998. Washington D.C.*
2. *G.I. Obiefuna, A. Sheriff (2011). Assessment of Shallow Ground Water Quality of Pindiga Gombe Area, Yola Area, NE, Nigeria for Irrigation and Domestic Purposes.*
3. *Gupta DP, Sunita and Saharan JP (2009) Physiochemical analysis of groundwater of selected area of Kaithal City (Haryana) India. Researcher, 1(2), 1-5.*
4. *Gupta, B. K. and R. R. Gupta. (1999). Physio-chemical and biological study of drinking water in Satna, Madhya Pradesh. Poll. Res., 18, 523-525.*
5. *Rajan M. R. and I. Paneerselvam. (2005). Evaluation of drinking water quality in Dindigul city, Tamil Nadu. Indian J. Environ. and Ecoplan. Vol. 10, No.3, 771-776.*
6. *Rajas Kara Pandian, M., G. Sharmila Banu, G. Kumar and K. H. Smila. (2005). Physico-chemical characteristics of drinking water in selected areas of Namakkal town (Tamil Nadu), India. Indian J. Environmental Protection, 10 (3), 789-792.*
7. *Ravisankar N and Poogothai S (2008) A study of groundwater quality in Tsunami affected areas of sirkazhi taluk, Nagapattinam district, Tamilnadu, India. Sci. Tsunami Hazards, 27(1), 47-55.*
8. *Singh VS, Thangarajan M (2004). Determination of shallow aquifer parameters in Kodaganar River Basin, Dindigul and Karur Districts, Tamil Nadu. Jour. Geol. Soci. India, 64 (6), 763-774.*
9. *Majumdar PK, Ghosh NC, Chakravorty B (2002). Analysis of arsenic contaminated groundwater domain in the Nadia district of West Bengal (India). Hydrol. Sci. Jourl., 47(S), S 55-66.*

Probability Distribution Function of Turbulence Parameter in Curvilinear Cross Section Mobile Bed Channel

Anurag Sharma[1], Bimlesh Kumar[2]

[1]*Postgraduate student, Department of Civil Engineering, Indian Institute of Technology Guwahati, India-781039, anurag.sharma@iitg.ac.in*

[2]*Assistant Professor, Department of Civil Engineering, Indian Institute of Technology Guwahati, India-781039, 0091-361-2582420, bimk@iitg.ac.in*

ABSTRACT

The present study investigates the probability density functions (PDFs) of two dimensional turbulent velocity fluctuations and Reynolds shear stress in open channel flow over rough beds are obtained using a Gram–Charlier (GC) series expansion based on the exponential distribution. The GC series expansion has been used up to the moments of order four to include the skewness and kurtosis. the Experiment was carried out on the curvilinear cross section sand bed channel at threshold condition with uniform sand size of d50=0.418mm. The result concludes that the PDFs distributions of turbulent velocity fluctuations and Reynolds shear stress calculated theoretically based on GC series expansion satisfied the PDFs obtained from the experimental data.

Keywords: Open channel flow; Probability density function; Stream wise velocity; Vertical velocity.

1. Introduction

The fluctuation of stream wise and vertical velocity u' and w' are the random quantities in open channel flow whose mean value of the product u' w' yields the Reynolds shear stress where ρ is the density of water. Due to this reason, in a flowing fluid is nonzero implies that u' and w' are correlated quantities. The theoretical analysis of this random quantities u' and w' are well explained by the simple one sided exponential distribution of probability function. The Probability Distributions are derived from a truncated universal Gram Charlier series expansion based on the exponential or Laplace type distributions for turbulent velocity fluctuations. The knowledge of Probability density function (PDF) of these quantities helps in understanding the associated turbulent bursting phenomenon (Nakagawa and Nezu 1977; Afzal et al. 2009). Frenkiel and Klebanoff (1967) and van Atta and Chen (1968) forecast that moments of u' is greater than two. By considering correlations at two points separated in time, they have delineated that even-order correlations can be achieved by assuming a Gaussian joint PDF while the odd-order correlations follow a Gaussian based Gram.Charlier (GC) PDF. Antonia and Atkinson (1973) have considered non-Gaussian behaviour of u' and w' to use a GC series expansion for the joint PDFs of u' and w' obtained by inverting a Gaussian based characteristics function.

The series was curtailed by eliminating cumulants of order higher than four to maintain skewness and flatness. Nakagawa and Nezu (1977) considered a GC based joint PDF in the form given by kampe de Feriet (1966). Bose and Dey (2010) observed the theoretical expression for the PDF of u', w' and u'w' which is derived from a GC series based on the exponential distribution and also reflecting skewness and Kurtosis in the distribution. They have also constructed the conditional PDFs of u'w' and validated by experimental data for smooth and rough bed. The prevalence of bursting events in the near-bed flow zone provokes non-Gaussian PDF distributions for the turbulent quantities (Bose and Dey 2010).

Despite from a number of series of efforts, the PDFs of random turbulence quantities in case of curvilinear cross section mobile bed channel condition is still yet to be ascertained. Probability density function (PDF) of a continuous random variable is a function that describes the relative likelihood for this random variable to take on a given value. The concept of the probability distribution and the random variables which they describe underlies the mathematical discipline of probability theory, and the science of statistics.. In the present research work, curvilinear cross section mobile bed streams used to collect experimental data that has been employed to investigate probability distribution function of turbulence parameters theoretically and experimentally and compare in between them. This study is in fact an extension of the study by Sharma et al. (2015) on mobile-bed flows.

2. Experimental Program

In the present work, experiment was done in a large tilting flume with dimensions of 17.24 m in length, 1m in width, and 0.72m in deep (Figure 1).

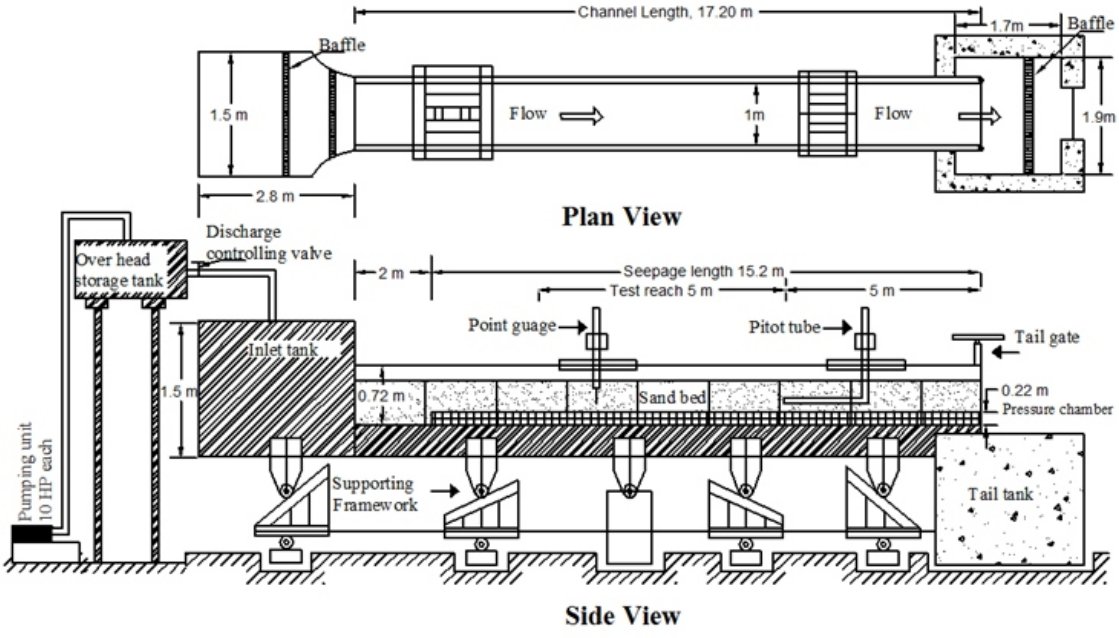

Figure 1 Schematics diagram of large tilting flume

A tank of dimensions 2.8 m long, 1.5 m wide and 1.5 m deep is provided at the upstream of the flume which serves to straighten the flow prior to its introduction in to the flume. The upstream tank gets water through the overhead tank where water is pumped by three pumps of 10 HP capacities each. A control valve is located at the overhead tank and is used to regulate the flow in the main channel. A wooden baffle is installed in the upstream tank which prevents turbulences in the water coming from the overhead tank, to enter the main channel. A tail gate is provided at the downstream end of the main channel which can be raised or lowered to control the flow depth. The tail gate is operated manually by a geared mechanism with edges, which allows precise positioning of the gate. A tank is provided at the downstream of the flume to collect the water from channel and release it to the underground trench, which delivers it to an underground tank from where the water is pumped into the overhead tank. This way the water is recirculating in the experiment. Flow discharge from the main channel has been measured by recording the depth of flow over the rectangular notch provided at the downstream collection tank. Water is introduced to the channel by gradually opening a valve located at the overhead tank. After the bed was completely submerged, the tail gate is adjusted in such a way that there is bank full flow in the channel. At the same time, the upstream discharge was adjusted so that the incipient condition is reached when all fractions of bed particles (on the surface) initiate movement over a period of time. Once the incipient condition is reached, discharge Q and corresponding flow depth y are registered. In incipient motion condition, bed shear stress and critical shear stress are nearby equal. Visual observation was made to cross check the threshold motion suggested by Yalin (1976). Shield's (1936) diagram was also used to confirm the threshold condition. For given sediment size, the flow condition corresponding to the region above the curve represents sediment motion, while the region below the curve refers to no sediment motion.

Most of the stable channel predictors are empirical or semi-empirical in nature except the one proposed by Lane (1953). Empirical predictors are developed based on the experimentation and usually valid within the ranges of parameters of the experiments. The theoretical regime equation developed by Lane (1953) has been derived by solving various forces those can act on the sediment-water flow. Curvilinear profile of Lane's shape was prepared with the help of wooden shaper. Relations between flow depth (y_0), area (A), velocity (u) and top width (B) for a stable channel cross-section have been given by Lane (1953) as:

$$A = \frac{2y_0^2}{\tan\varphi} \tag{1}$$

$$u = \frac{1}{n}\left[\frac{y_0 \cos\varphi}{E(\sin\varphi)}\right]^{2/3} S^{1/2} \tag{2}$$

$$B = \frac{y_0 \pi}{\tan\varphi} \tag{3}$$

$$E(\sin\varphi) \approx (\pi/2)\left(1 - 1/4\sin^2\varphi\right) \tag{4}$$

$$y = y_{max} \cos\left\{\left(\frac{\tan\varphi}{y_{max}}\right)x\right\} \tag{5}$$

Shape of the main channel has been given using equation (5). *Lane's* (1953) geometric profiles with 0.70 m (shape 70) were used. For shape 70, maximum depth (0.142 m) of flow can be calculated by rearranging equation. Flow measurements have been taken at a test section of 7.5 m from the inlet during experimental run. The experiment were conducted by maintaining the incipient motion discharge (Q) of 0.0169 m^3/sec, flow depth (h) of 0.14m and bed slope (S_0) of 0.0015.

Three dimensional water velocity measurements in the main channel are taken by Vectrino Acoustic Doppler Velocimeter (ADV) obtained from Nortek. The Vectrino uses the Doppler Effect to measure current velocity. The Vectrino transmits short pairs of sound pulses, listens to their echoes, and ultimately measures the change in pitch or frequency of the returned sound. ADV makes sampling volume at a vertical distance of 5cm from the central transmitter while components of velocity were sampled in the remote sampling volume at the rate of 200 Hz for the duration of 120 seconds. Sampling duration was increased to 200 sec near the bed for better understanding of integral scale and turbulent statistics. The flow depth of water in to the channel is measured with the help of a digital point gauge attached to a moving trolley. This is a direct indicating gauge which eliminates observation errors due to Vernier and scale reading. It can be set to zero anywhere in the operating range to permit easy relative level checking. The liquid crystal display is easy to read and has a resolution of ±0.01mm. A quick-release mechanism permits rapid changes of position. The depth of flow is defined as a difference between the water surface level and the bed level. Average temperature of water during an experiment is recorded by Vectrino Acoustic Doppler Velocimeter which has a temperature sensor (thermistor), located inside the probe head. The corresponding value of kinematic viscosity (cm^2/s) is determined from standard tables. Water surface slope in experiments is measured using a Pitot-static tube connected to a digital manometer which is further attached to a moving trolley.

The digital manometer is powered by two batteries of 12 Volts each connected in series. The outer tube consisting static pressure holes when connected to digital manometer gives the piezometric height at that point. This way moving along the channel in the longitudinal direction, water surface slope is measured. Bed slope (S_0) of the flume is measured by using total station.

3. Post Processing of Velocity Data

Signal to noise ratio (SNR) and correlation has been used for filtering the velocity data points. In the experiment, SNR and correlation was kept as minimum 15 and 70 respectively. Near the bed, correlation was reduced to 65 (Dey *et al*. 2012). The data measured from the vectrino contained spikes so the data were filtered by a spike removal algorithm based on the acceleration thresholding method (Goring and Nikora 2002). The threshold value was maintained in between 1 to 1.5 so that velocity power spectra should acceptable fit with Kolmogorov "-5/3 scaling law" in the inertial sub range (Lacey and Roy 2008).Velocity power spectra $F_{ii}(f)$ at z=0.05m are presented in the Figure 2 where f is frequency and z is flow depth.

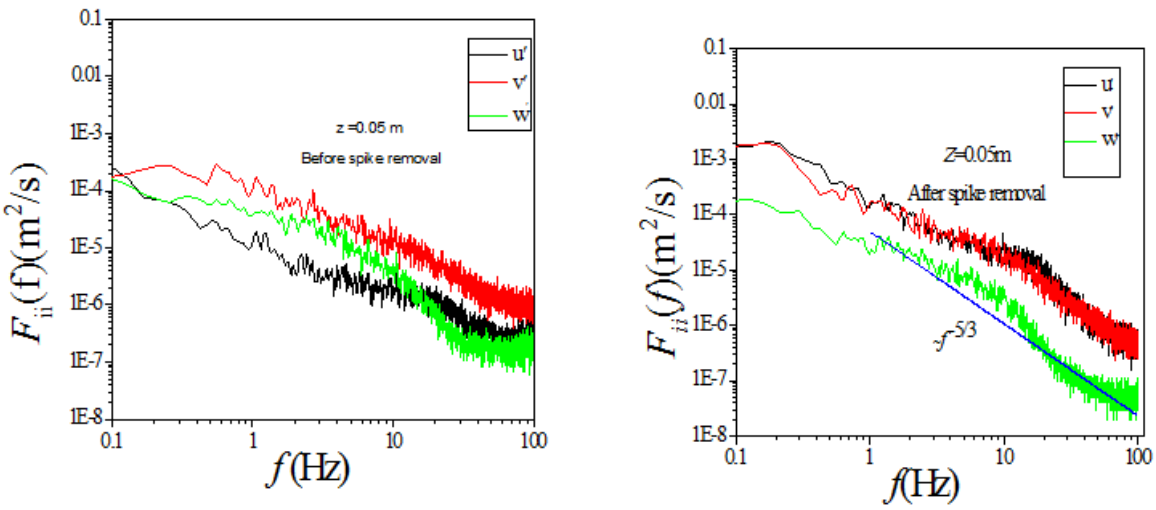

Figure 2 Velocity power spectra $F_{ii}(f)$ before and after spike removal

4. Results and Discussions

In open channel flow, Production of turbulence at near bed region is due to flow over the bed. The two dimensional instantaneous velocities (u,w) at a point can be decomposed in terms of time averaged part ($\bar{u}$, $\bar{w}$) and fluctuation part (u',w') by applying Reynolds decomposition in the way (u,w) = ($\bar{u}$,$\bar{w}$) + (u',w'). Bose and Dey (2010) and Dey et al.(2012) shows that velocity fluctuation (u',w')

follows the Gram Charlier (GC) series based on exponential distribution at which u' and w' is normalized as $\hat{u} = \frac{u'}{\sigma_u}$ and $\hat{w} = \frac{w'}{\sigma_w}$ where, σ_u and σ_w are the stream wise and vertical turbulence intensity respectively. Bose and Dey (2010) has given the probability density function (PDF) for stream wise and vertical velocity fluctuation as explained in the following form of equations.

$$P_{\hat{u}}(\hat{u}) = \left[\begin{array}{l} \frac{1}{2} + \frac{1}{4}C_{10}\hat{u} - \frac{1}{16}C_{20}(1 + |\hat{u}| - \hat{u}^2) - \frac{1}{96}C_{30}\hat{u}(3 + 3|\hat{u}| - \hat{u}^2) \\ + \frac{1}{768}C_{40}(9 + 9|\hat{u}| - 3\hat{u}^2 - 6|\hat{u}|^3 + \hat{u}^4) + ... \end{array}\right] \exp(-|\hat{u}|) \quad (6)$$

$$P_{\hat{w}}(\hat{w}) = \left[\begin{array}{l} \frac{1}{2} + \frac{1}{4}C_{01}\,\hat{w} - \frac{1}{16}C_{02}(1 + |\hat{w}| - \hat{w}^2) - \frac{1}{96}C_{03}\,\hat{w}(3 + 3|\hat{w}| - \hat{w}^2) \\ + \frac{1}{768}C_{04}(9 + 9|\hat{w}| - 3\,\hat{w}^2 - 6|\hat{w}|^3 + \hat{w}^4) + ... \end{array}\right] \exp(-|\hat{w}|) \quad (7)$$

Where, $C_{10} = m_{10}$, $C_{20} = \frac{1}{2}m_{20} - 1$, $C_{30} = \frac{1}{6}m_{30} - 2m_{10}$, $C_{40} = \frac{1}{24}m_{40} - \frac{3}{2}m_{20} + 2$

$C_{01} = m_{01}$, $C_{02} = \frac{1}{2}m_{02} - 1$, $C_{03} = \frac{1}{6}m_{03} - 2m_{01}$, $C_{40} = \frac{1}{24}m_{40} - \frac{3}{2}m_{20} + 2$

Where, $m_{j0} = \int_{-\alpha}^{\alpha} \hat{u}^j P_{\hat{u}}(\hat{u})\,\mathrm{d}\hat{u}$, $m_{0k} = \int_{-\alpha}^{\alpha} \hat{w}^j P_{\hat{w}}(\hat{w})\,\mathrm{d}\hat{w}$ (Bose and Dey 2010). As a result, the coefficient

C_{j0} and C_{0k} is to be estimated from the experimental data. The theoretical curves for PDF s of $P_{\hat{u}}(\hat{u})$ and $P_{\hat{w}}(\hat{w})$ can be estimated by using the relative frequency $f_{\hat{u}}(\hat{u})$ and $f_{\hat{w}}(\hat{w})$ of the random variables û and ŵ which was determined from the experimental data at a given flow depth z. The moment m_{j0} and m_{0k} were estimated by approximating $P_{\hat{u}}(\hat{u})$ and $P_{\hat{w}}(\hat{w})$ by $f_{\hat{u}}(\hat{u})$ and $f_{\hat{w}}(\hat{w})$ respectively and the integrals were evaluated by a composite Simpson's rule. In this way, the C_{j0} and C_{0k} were estimated by using Equation (6) and (7) and the PDFs are computed to yield the theoretical curves for $P_{\hat{u}}(\hat{u})$ and $P_{\hat{w}}(\hat{w})$. One point on a vertical line have been selected for the study of PDFs $P_{\hat{u}}(\hat{u})$ and $P_{\hat{w}}(\hat{w})$. They are at within the inner layer (z=0.18h). Figure 3 shows $P_{\hat{u}}(\hat{u})$ and $P_{\hat{w}}(\hat{w})$ distributions at the inner layer. The coefficient C_{j0} and C_{0k} are tabulated in Table 1.

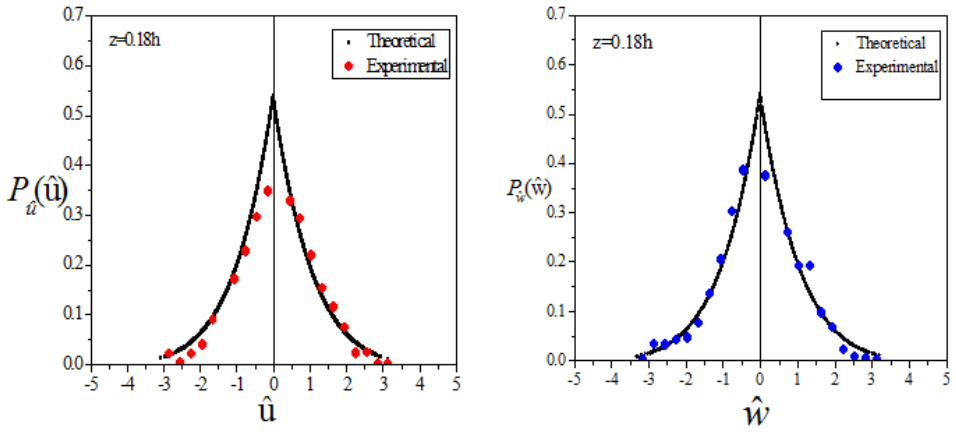

Figure 3 Comparisons of computed $P_{\hat{u}}(\hat{u})$ and $P_{\hat{w}}(\hat{w})$ with experimental data

Table 1 Coefficient for the computation of $P_{\hat{u}}(\hat{u})$ and $P_{\hat{w}}(\hat{w})$

Case	C_{10}	C_{01}	C_{20}	C_{02}	C_{30}	C_{03}	C_{40}	C_{04}
z = 0.18h	0.00023	-0.0012	-0.5	-0.5	-0.0051	-0.05	0.611	0.632

Experimental data correspond to calculate $P_{\hat{u}}(\hat{u})$ and $P_{\hat{w}}(\hat{w})$ collapsing reasonably on the computed curves, implying that $P_{\hat{u}}(\hat{u})$ and $P_{\hat{w}}(\hat{w})$ can be represented by GC series expansion based on exponential distribution. The computed $P_{\hat{u}}(\hat{u})$ and $P_{\hat{w}}(\hat{w})$ distributions are sharply peaked at zero velocity fluctuations that is not observed in case of experimentally estimated PDFs distributions because of the absence of relative frequencies of such narrow ranges in the Histogram. The results pointed that PDFs distributions for velocity fluctuations derived from GC series expansion based on exponential distributions follows their universality being applicable to mobile bed flows.

Reynolds Shear stress (RSS) is defined by $\tau = -\rho\overline{u'w'}$ hence $-\frac{\tau}{\rho}$ is the mean value of product of random variable u'w' due to which the PDFs of τ depends upon the joint PDFs of u' and w'. In order to study the PDFs of τ, Consider dimensionless random variable $\hat{\tau} = \hat{u}\hat{w}$. Based on this consideration, Bose and Dey (2010) derived the PDFs of $\hat{\tau}$ as

$$
\begin{aligned}
P_{\hat{\tau}}(\hat{\tau}) &= K_0(2\tau_1) - \frac{1}{8}(C_{20}+C_{02})(1-\tau_1^2)K_0(2\tau_1) \\
&+ \frac{1}{4}C_{11}\hat{\tau}K_0(2\tau_1) + \frac{1}{64}C_{22}\left[(1-\tau_1^2+\tau_1^4)K_0(2\tau_1) - 2\tau_1^3K_1(2\tau_1)\right] \\
&- \frac{1}{96}(C_{31}+C_{13})\hat{\tau}(3-\tau_1^3)\left[K_0(2\tau_1)+\tau_1K_1(2\tau_1)\right] \\
&+ \frac{1}{384}(C_{40}+C_{04})\left[(9-9\tau_1^2+\tau_1^4)K_0(2\tau_1) - 2\tau_1^3K_1(2\tau_1)\right] + \ldots\ldots
\end{aligned}
\tag{8}
$$

Where $\tau_1 = \left(|\hat{\tau}|\right)^{0.5}$, K_0 and K_1 are the Bessel function of order 0 and 1 respectively. The coefficient in the above expression can be found out by the following moments

$$\int_{-\infty}^{\infty} \hat{\tau} P_{\hat{\tau}}(\hat{\tau}) d\hat{\tau} = C_{11} + \frac{11}{8}(C_{31} + C_{13})$$

$$\int_{-\infty}^{\infty} \hat{\tau}^2 P_{\hat{\tau}}(\hat{\tau}) d\hat{\tau} = 4 + 4(C_{20} + C_{02}) + \frac{25}{4} C_{22}$$

$$\int_{-\infty}^{\infty} \hat{\tau}^3 P_{\hat{\tau}}(\hat{\tau}) d\tau = 144 C_{11} + 7407(C_{31} + C_{13})$$

Where, $C_{20} = \frac{1}{2} m_{20} - 1$, $C_{02} = \frac{1}{2} m_{02} - 1$, $C_{40} = \frac{1}{24} m_{40} - \frac{3}{2} m_{20} + 2$ $C_{40} = \frac{1}{24} m_{40} - \frac{3}{2} m_{20} + 2$

The theoretical curves for PDFs of $P_{\hat{\tau}}(\hat{\tau})$ is estimated by using the relative frequency $f_{\hat{\tau}}(\hat{\tau})$ by replacing $P_{\hat{\tau}}(\hat{\tau})$ of the random variables ûŵ which was determined from the experimental data at a given flow depth z. The required parameters are calculated to yield the theoretical expression for $P_{\hat{\tau}}(\hat{\tau})$ given by equation (8). Figure 4 compare computed and observed $P_{\hat{\tau}}(\hat{\tau})$ distributions at inner layer z=0.18h. The values of coefficient are tabulated in Table 2.

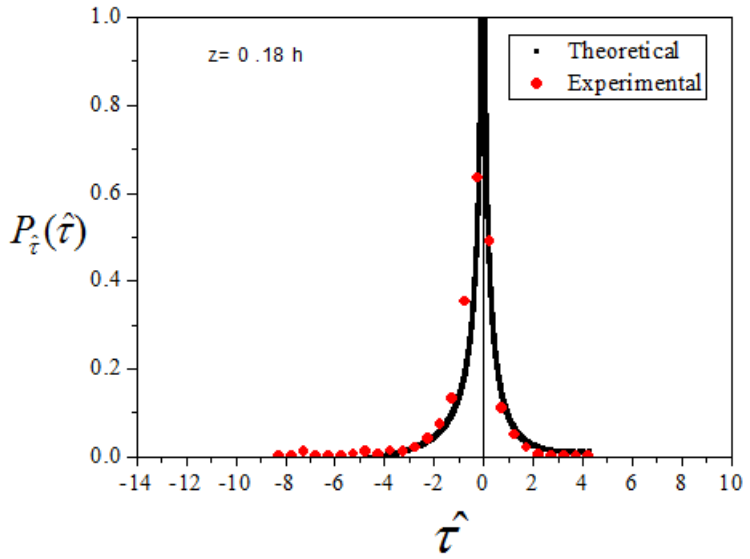

Figure 4 Comparisons of computed $P_{\hat{\tau}}(\hat{\tau})$ with experimental data

Table 2 Coefficient for the computation of $P_{\hat{\tau}}(\hat{\tau})$

Case	C_{11}	C_{13}	C_{31}	C_{22}
$z = 0.18h$	-0.40	0.59	0.616	0.34

Figure 4 indicate that the experimental data are in good agreement with the computed curves implies that derivation of $P_{\hat{\tau}}(\hat{\tau})$ using the GC series expansion based on the exponential distribution being applicable to mobile-bed flows.

4. Conclusions

The PDF distributions of u′, w′, and u′w′ are calculated theoretically using a GC series expansion based on the exponential distribution truncating the series up to fourth order. The computed and experimental PDF distributions are in good agreement which indicates that the calculation of probability density function of fluctuating component of velocity and Reynolds shear stress by Gram Charlier series based on exponential distribution being applicable for mobile bed flows.

5. References

Afzal, B., Faruque, M.A., and Balachandar, R. (2009). Effect of Reynolds number, near-wall perturbation and turbulence on smooth open-channel flows. J. Hydraulic Res., 47(1), 66–81.

Antonia, R.A., and Atkinson, J.D. (1973). High-order moments of Reynolds shear stress fluctuations in a turbulent boundary layer. J. Fluid Mech., 58, 581–593.

Bose, S.K., and Dey, S. (2010). Universal probability distributions of turbulence in open channel flows. J. Hydraul. Res., 48(3), 388-394.

Dey, S., Das, R., Gaudio, R., and Bose, S.K. (2012). Turbulence in mobile bed streams for flat bed. Acta Geophysica, 60(6), 1547-1588.

Frenkiel, F.N., and Klebanoff, P.S. (1967). Higher order correlations in a turbulent field. Phys. Fluids. 10(3), 507–520.

Goring, D.G., and Nikora, V.I. (2002). Despiking acoustic Doppler velocimeter data. J. Hydraul. Eng., 128(1), 117-126.

Kampe´ de Fe´riet, J. (1966). The Gram-Charlier approximation of the normal law and the statistical description of homogenous turbulent flow near statistical equilibrium. David Taylor Model Basin Report 2013. Naval Ship Research and Development Center, Washington, DC.

Lacey, R.W.J., and Roy, A.G (2008). Fine-scale characterization of the turbulent shear layer of an in stream pebble cluster. J. Hydraul. Eng., 134(7), 925-936.

Lane, E.W. (1953). Progress report on studies on the design of stable channels by the bureau of reclamation. Proceedings, ASCE, 79, Separate 280, 1-31.

Nakagawa, H., and Nezu, I. (1977). Prediction of the contributions to the Reynolds stress from bursting events in open-channel flows. J. Fluid Mech,. 80, 99–128.

Nezu, I., and Nakagawa, H. (1993). Turbulence in Open-Channel Flows. Balkema, Rotterdam.

Sharma, A., Patel, M., and Kumar, B. (2015). Turbulent parameters and corresponding sediment transport in curved cross section channel. ISH J. Hydraul. Eng.

Shields, A. (1936). Application of similarity principles and turbulence research to bed-load movement. California Institute of Technology, Pasadena, CA.

Van Atta, C.W., and Chen, W.Y. (1968). Correlation measurements in grid turbulence using digital harmonic analysis. J. Fluid Mech., 34, 497–515.

Yalin, M.S. (1976). Mechanics of sediment transport. Pergamon, Oxford, U. K.

Spatial Analysis For Optimum Design of Observation Network of Wells In Watershed Within Diverse Aquifer Using Geostatistics Integrated With GIS

Chandan Kumar Singh[1], Yashwant B.Katpatal[2]

[1]*PhD Student, Department of Civil Engineering, VNIT Nagpur-440 01, India*

[2]*Professor, Department of Civil Engineering, VNIT Nagpur-440 010, India*

singhchandan44@gmail.com, *ybkatpatal@rediffmail.com*

+91 9422303373, +91 9595237501

ABSTRACT

Groundwater is the important natural resource used for agriculture, domestic and industrial purposes. As the dependence on groundwater has increased over the years, it can create imbalance in its availability which may lead to overexploitation of this resource. Major part of the agriculture and rural water supply requirements are met from groundwater. Hence, the sustainable development of groundwater resources should be ensured through proper assessment supported by strong database. Groundwater level monitoring is one of the important exercises which is carried out by several central and state government agencies in the country and through which the most important observation data is collected which helps in groundwater management. In this regard, the well selections for observation become important to have optimally justifiable data. It has been observed while using the groundwater level data for modeling that the data in terms of number of wells observed is not sufficient to understand and represent the correct groundwater scenario in many areas. The groundwater levels of observation wells are known for all the monitored location, but the water level values for other unmonitored locations are also of interest and it must be considered. However, due to cost and practicality, monitoring stations cannot be placed everywhere. The objective of the present study is to perform spatial analysis for optimum location of observation wells for monitoring of groundwater resources, especially in rural areas. Groundwater level data has been obtained from the observation wells of Wainganga sub-basin Nagpur District, Maharashtra, India. Nagpur district has varied geological set up; it has all the rocks types like igneous, sedimentary and metamorphic. Out of 40 sub-watersheds present in the Wainganga sub basin, 18 sub-watersheds are selected based on the geological formation and number of observation wells. Geographical Information System has been used for generating the suitable sites for observation wells. Kriging interpolation technique of geostatistical method is compared with deterministic method to interpolate groundwater levels in unobserved locations of study area. The spatial distribution of groundwater levels and its associated error variances is computed and the location having maximum error variances are selected as additional sites for extending the existing network of wells.

Keywords: Groundwater, Observation wells, Kriging interpolation, Watersheds, Aquifer.

1. Introduction

The objective of present study is to optimize the groundwater level monitoring network efficiently and accurately for estimation of groundwater resources and agriculture planning within watershed. Groundwater monitoring generally starts at small scale with local problems. It evolves into regional or national monitoring networks focusing on both of local and regional problems (Zhou et al., 2013). There are different classifications of groundwater level monitoring networks (WMO, 1989; UNESCO, 1998; Jousma and Roelofsen, 2004). Two main types of groundwater level monitoring networks are generally followed which are basic monitoring networks and specific monitoring networks. Basic groundwater level monitoring network involves monitoring for larger area; whole country wise or complete basin wise. Observation wells are installed at relatively larger distances and frequency of observation is low for infinitely long period. Specific monitoring networks are designed for local scale focused on specific purposes, for example, decline in groundwater table for irrigation, domestic water supply, natural conservation areas etc. It is not possible to select the sample observation well everywhere and to achieve this objective, networks of well should be optimum and can be selected on the basis of scientific methods. It is observed that large number of publications are available on designing groundwater quality monitoring networks and there are significantly less publications on designing groundwater level monitoring networks (ASCE, 2003). In past decades, number of methods have been implemented from time to time by different researchers and agencies for groundwater level monitoring based on Geostatistical, Hydrogeology, Numerical modeling, Geographical Information System etc. Zhou et al. (2013) applied groundwater regime zone mapping method and considered various spatial factors which can influence groundwater monitoring. Geographical Information System is a tool that can be used effectively for groundwater regime zone mapping. Interpolation methods such as inverse distance weighting (IDW) and kriging have been widely applied for groundwater level mapping (Varouchakis and Hristopulos 2013; Theodossiou and Latinopoulos 2006; Ahmadi and Sedghamiz 2007; Yang et al. 2008; Prakash and Singh 2000). Sophocleous et al. (1982) applied universal kriging to study groundwater level monitoring network of Northwest Kansas. It is difficult to select the optimum number of observation wells due to heterogeneous nature of the aquifers and varied Hydrogeological parameters. In the present study deterministic and geostatistical methods have been used to select the optimum number of observation wells for groundwater level monitoring in Waninganga sub-basin within Nagpur district boundary and it is observed that geostatistical method is more accurate as compared to deterministic method.

2. Materials and methods

2.1 Study area

Wainganga sub basin is selected as study area which is in Nagpur district of Maharashtra, India. It lies between north latitudes 20°35' and 21°44' and east longitudes 78°15' and 79°40' and falls in Survey on India topo-sheets 55 K, O and P, with an elevation about 310 m above mean sea level. Kanhan and Pench are the main rivers flowing through the district. Major crops in entire district are jowar, cotton, wheat and pulses and the normal annual rainfall is around 1000 mm to 1200 mm. Wainganga sub-basin has 40 sub-watersheds within Nagpur district out of which 18 sub-watersheds are selected for study (Figure 1) and its total geographical area is approximately equal to 3320 km^2. It was selected on the basis of different geologic formation and adequate number of observation wells for the purpose of designing observation networks of wells. Nagpur district has varied geological set up; it has all the rocks types like igneous, sedimentary and metamorphic. Observation well data for 18 sub-watersheds were obtained from CGWB (Central Ground Water Board) and GSDA (Groundwater Surveys and Development Agency).

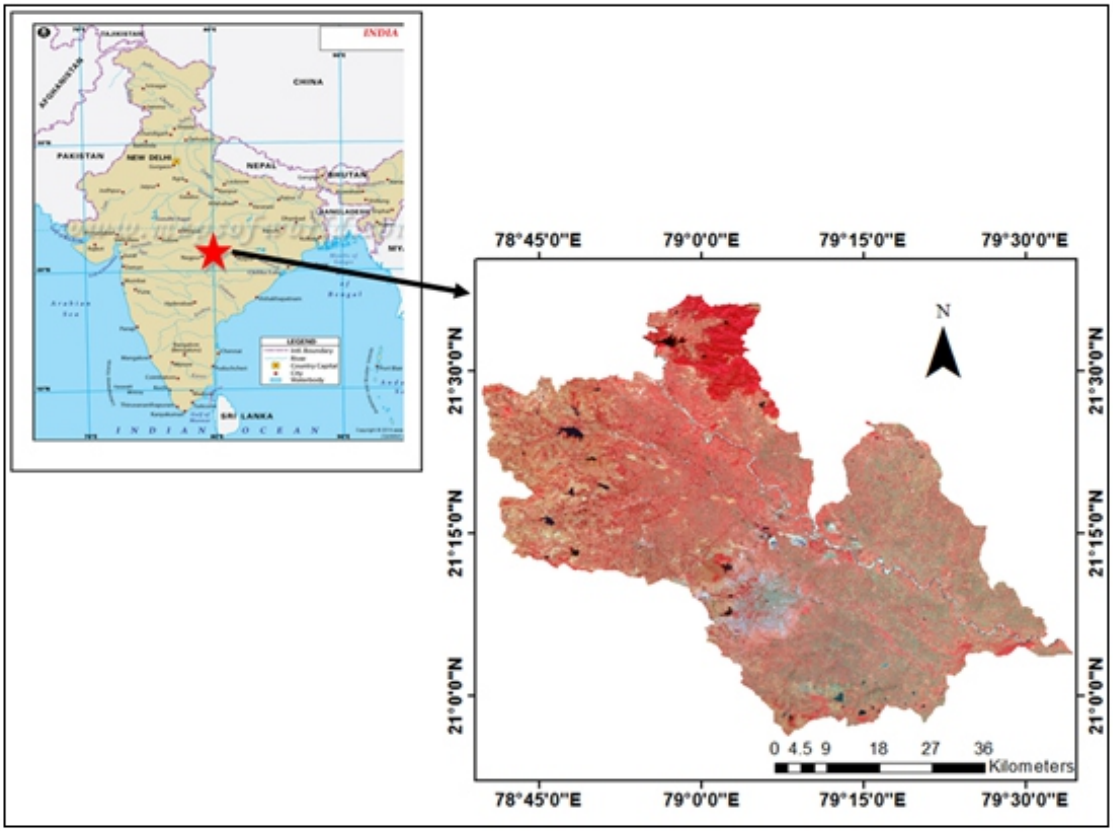

Figure 1 Location map of study area

2.2 Geostatistical method

Geostatistics can be defined as the branch of statistical sciences that studies spatial/temporal phenomena and capitalizes on spatial relationships to model possible values of variables at unobserved, unsampled locations (Caers, 2005). Geostatistical methods that are based on statistical models include autocorrelation (statistical relationships among the measured points). Not only do these techniques have the capability of producing a prediction surface, but they can also provide some measure of the certainty or accuracy of the predictions. To predict values and assess the uncertainty at unmeasured locations, Kriging interpolation has been used. It can be used to produce maps of predicted values, standard errors associated with predicted values. Complete discussions of kriging methods and their explanation can be found in Goovaerts (1997). The general equation of kriging estimator is

$$Z^*(x_p) = \sum_{i=1}^{n} \lambda_i Z(x_i) \quad (1)$$

In order to achieve unbiased estimations in kriging, the following set of equations should be solved simultaneously.

$$\begin{cases} \sum_{i=1}^{n} \lambda_i \gamma(x_i, x_j) - \mu = \gamma(x_i, x) \\ \sum_{i=1}^{n} \lambda_i = 1 \end{cases} \quad (2)$$

where $Z^*(x_p)$ is the kriged value at location (x_p), $Z(x_i)$ is the known value at location x_i, λ_i is the weight associated with the data, μ is the Lagrange multiplier and $\gamma(x_i, x_j)$ is the value of variogram corresponding to a vector with origin in x_i and extremity in x_j

2.3 Deterministic method

Deterministic methods are based on parameters that control either the extent of similarity of the values or the degree of smoothing in the surface. These techniques do not use a model of random spatial processes. Inverse distance weighting (IDW) is a deterministic method used in this study. The basis for the (IDW) interpolation technique, as its name implies, the weight of a value decreases as the distance increases from the prediction location. The general form of IDW (Shepard, 1968) method for an interpolated value Z at a given point 'x' based on samples may be written as:

$$Z(x) = \frac{\sum_{i=1}^{n} w_i(x) z_i}{\sum_{i=1}^{n} w_i(x)}$$

$$w_i(x) = \frac{1}{d(x, x_i)^p} \quad \text{if } d(x_i, x) \neq 0 \text{ for all } i \quad (3)$$

$$\text{if } d(x_i, x) = 0 \text{ for some } i$$

where $w_i(x)$ is a simple IDW weighting function, x denotes an interpolated (arbitrary) point, x_i is an interpolating (known) point, d is a given distance from the known point x_i to the unknown point x, n is the total number of known points used in interpolation and is a positive real number, called the power parameter.

Groundwater level in Wainganga sub basin for 18 sub watersheds were mapped and interpolated using geostatistical (ordinary kriging) and deterministic (inverse distance weighting) methods. Both these methods were implemented in GIS environment using geostatistical analyst tool. Groundwater level maps have been created separately using these two methods and it was compared to obtain the optimal solution. To access the accuracy, cross validation was performed. The interpolated values obtained from measured groundwater level data values were validated with the predicted values. Standard error map was prepared using ordinary kriging method and it was selected as the basis for augmenting additional number of observation well.

3. Results and discussion

Ordinary kriging and inverse distance weighting interpolation methods were applied to create groundwater level maps. Groundwater level data of 51 observation wells within study area were used to create maps (Figures 2 and 3) and the post monsoon season data for year 2011 was used to create map. Ordinary kriging and inverse distance weighting methods were applied based on (Equations 1, 2 and 3). Table 1 represents the comparisons of both deterministic and geostatistics methods where measured and predicted groundwater level values and cross validation results for both the methods are represented. Out of 51 observation wells most of the wells are located in NW and SE directions and fewer wells are in central part of the study area (Figure 3). Average groundwater levels in study area ranges from 2.15 to 7.8 m bgl (Figure 3). Groundwater levels observed were less in NW direction and increasing towards SE direction as shown in Figure 3. Surface elevation is higher in NW direction and slopes towards SE and hence it is authenticated that groundwater levels follows the general topography of the area and it validates that map created using interpolation methods are approximately correct up to a certain extent. It is observed that strong correlation exists between measured and predicted groundwater levels (Figure 5) estimated using ordinary kriging method; R^2 is calculated as 0.976. It is also observed that there is no correlation between measured and predicted groundwater levels (Figure 5) estimated using IDW method and R^2 is calculated as 0.045. The correlation is found to be more accurate for ordinary kriging because in this method weights used for predictions are based on distance between the measured points and the prediction location but also on the overall spatial arrangement of the measured points.

In IDW method negligible correlation is found because in this method weights used for predictions are based only on distance between the measured points and the prediction locations. Standard error map was created using measured and predicted values estimated using ordinary kriging method (Figure 6). Standard error map represents the spatial correlation between measured and predicted values; an error values decreasing close to zero indicates strong correlation between measured and predicted values and vice versa. Therefore, it can be considered for optimal solution for locating observation wells. In this study standard error map was created using 51 observation wells and it is found that error values ranges from 0.81 to 3.61. To obtain optimal solution, additional number of wells can be added at the location of high standard error and it is found that by adding additional number of wells errors value reduces. Addition of more number of wells results in reduction in standard error value. The number of wells at which standard error reaches its minimum value, with further addition of wells, there is no reduction in error value. At this point, it can be said that the network of wells has attained optimal solution and further addition of wells does not affect the change in error value. Number of additional wells responsible for reducing standard error can be selected for optimum design of groundwater level monitoring.

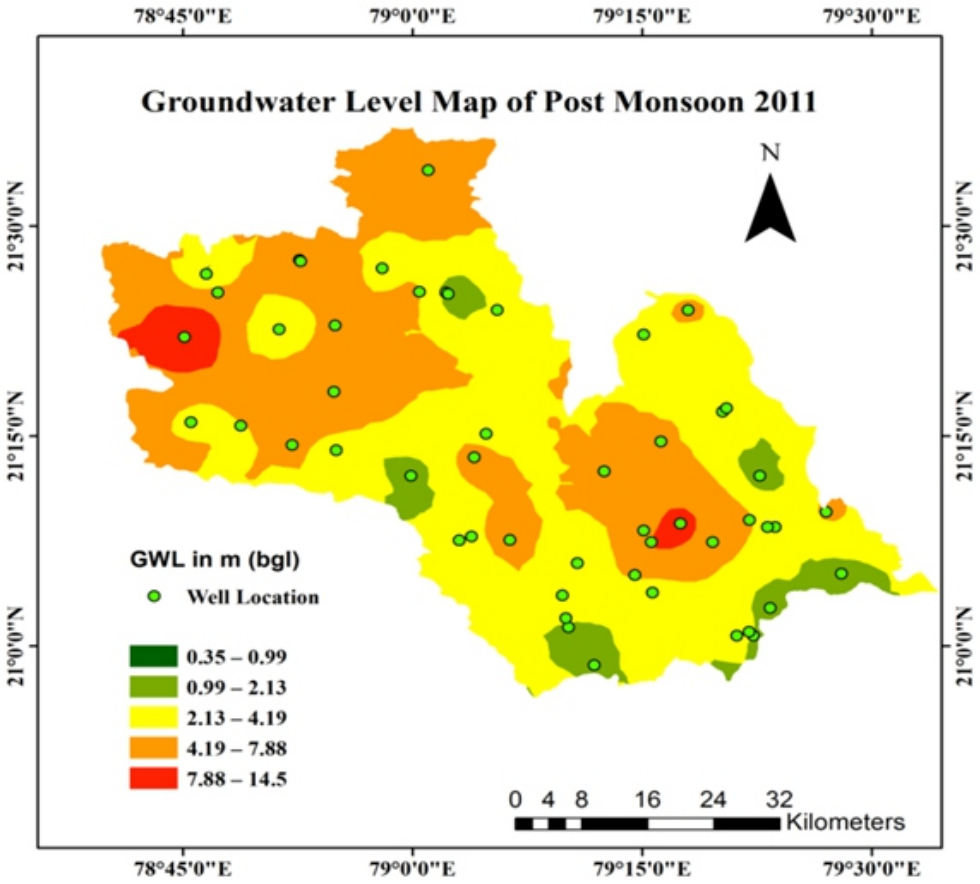

Figure 2 Groundwater level maps of Wainganga Sub-basin using Ordinary kriging method for post monsoon 2011

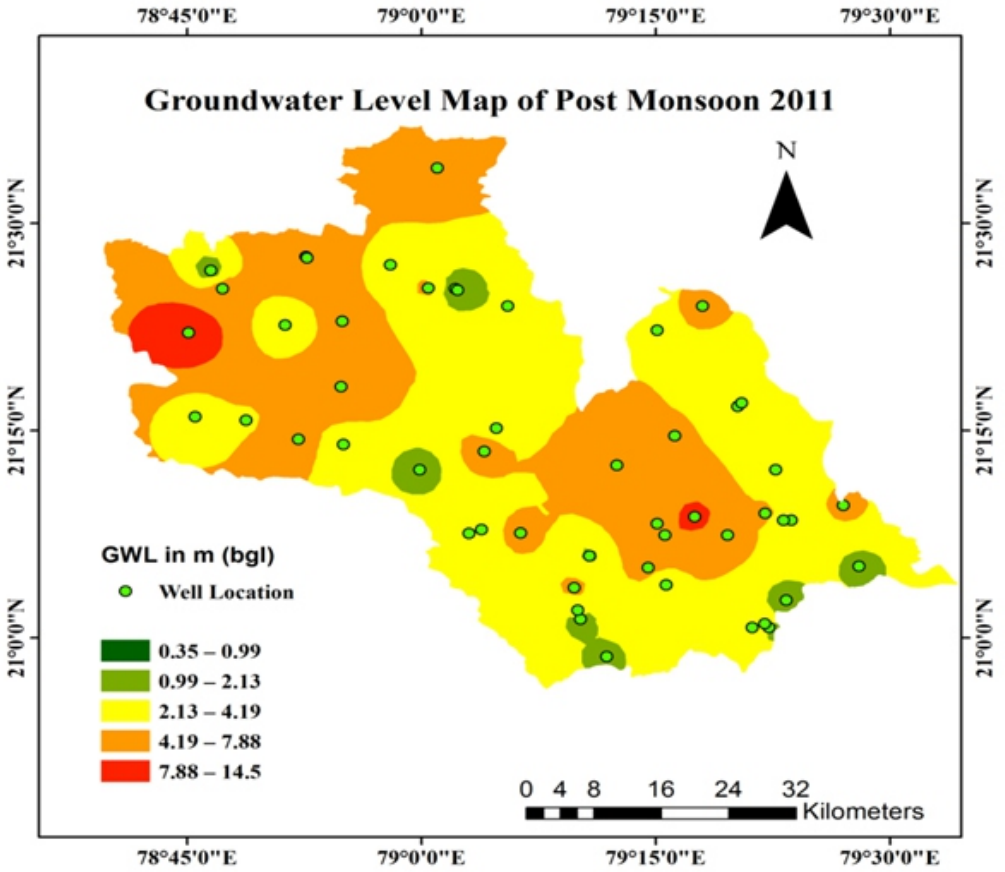

Figure 3 Groundwater level maps of Wainganga Sub-basin using Inverse Distance Weighted (IDW) method for post monsoon 2011

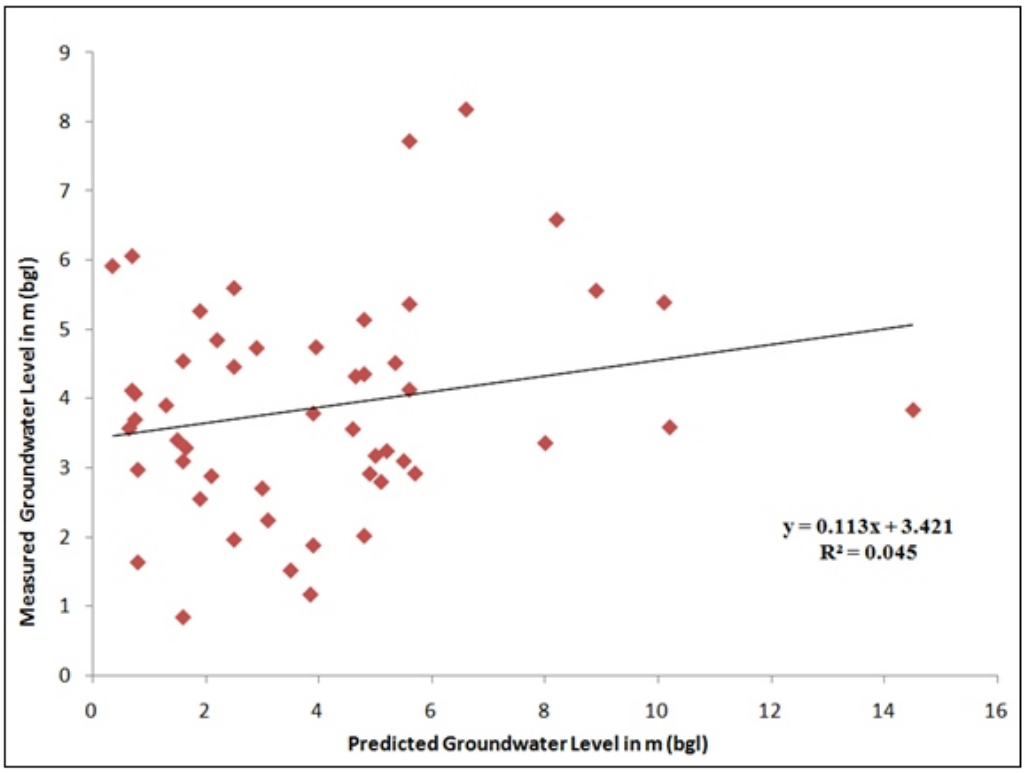

Figure 4 Scatter plot showing comparisons of measured vs. predicted groundwater levels of Wainganga Sub-basin using Kriging Interpolation method

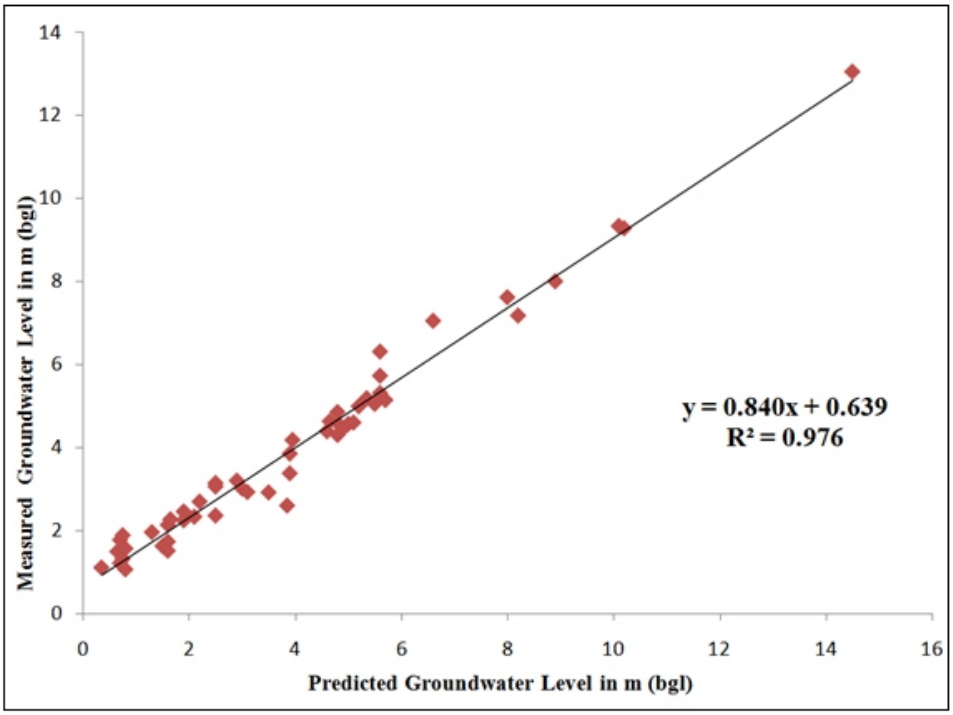

Figure 5 Scatter plot showing comparisons of measured vs. predicted groundwater levels of Wainganga Sub- basin using Inverse Distance Weighted (IDW) Interpolation method

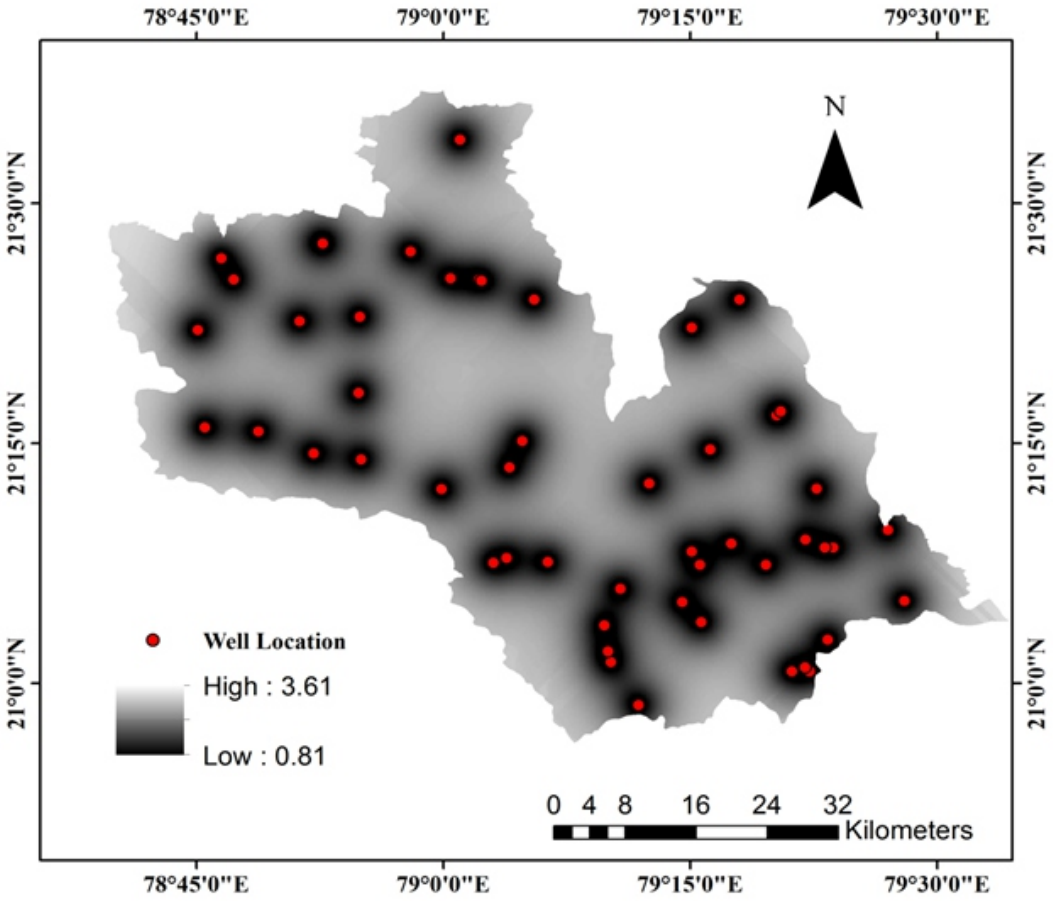

Figure 6 The standard error map coupled with kriged groundwater level of the study area

Table 1 Comparisons showing measured and predicted groundwater levels for post monsoon 2011, computed using geostatistical (ordinary kriging) and deterministic (Inverse distance weighting) methods and its associated errors

Obs. Well	Measured m (bgl)	Predicted m (bgl)		Errors		Obs. Well	Measured m(bgl)	Predicted m (bgl)		Errors	
		Kriging	IDW	Kriging	IDW			Kriging	IDW	Kriging	IDW
1	0.35	1.11	5.92	0.76	5.57						
2	0.65	1.50	3.57	0.85	2.92	27	3.9	3.85	3.79	-0.05	-0.11
3	0.7	1.77	6.07	1.07	5.37	28	3.9	3.38	1.88	-0.52	-2.02
4	0.7	1.22	4.12	0.52	3.42	29	3.95	4.18	4.75	0.23	0.80
5	0.75	1.32	4.07	0.57	3.32	30	4.6	4.39	3.56	-0.21	-1.04
6	0.75	1.89	3.70	1.14	2.95	31	4.65	4.63	4.33	-0.02	-0.32
7	0.8	1.07	2.98	0.27	2.18	32	4.8	4.30	2.02	-0.50	-2.78
8	0.8	1.57	1.64	0.77	0.84	33	4.8	4.59	4.36	-0.21	-0.44
9	1.3	1.96	3.91	0.66	2.61	34	4.8	4.85	5.14	0.05	0.34
10	1.5	1.63	3.40	0.13	1.90	35	4.9	4.45	2.92	-0.45	-1.98
11	1.6	1.73	3.10	0.13	1.50	36	5	4.57	3.18	-0.43	-1.82
12	1.6	2.14	4.55	0.54	2.95	37	5.1	4.60	2.80	-0.50	-2.30
13	1.6	1.51	0.84	-0.09	-0.76	38	5.2	4.99	3.25	-0.21	-1.95
14	1.65	2.27	3.29	0.62	1.64	39	5.35	5.18	4.52	-0.17	-0.83
15	1.9	2.25	2.55	0.35	0.65	40	5.5	5.05	3.10	-0.45	-2.40
16	1.9	2.46	5.27	0.56	3.37	41	5.6	6.31	7.73	0.71	2.13
17	2.1	2.33	2.88	0.23	0.78	42	5.6	5.73	5.37	0.13	-0.23
18	2.2	2.70	4.85	0.50	2.65	43	5.6	5.31	4.13	-0.29	-1.47
19	2.5	3.14	5.60	0.64	3.10	44	5.7	5.14	2.92	-0.56	-2.78
20	2.5	2.36	1.97	-0.14	-0.53	45	6.6	7.05	8.19	0.45	1.59
21	2.5	3.06	4.46	0.56	1.96	46	8	7.62	3.36	-0.38	-4.64
22	2.9	3.20	4.74	0.30	1.84	47	8.2	7.18	6.59	-1.02	-1.61
23	3	3.01	2.71	0.01	-0.29	48	8.9	8.00	5.56	-0.90	-3.34
24	3.1	2.93	2.24	-0.17	-0.86	49	10.1	9.33	5.39	-0.77	-4.71
25	3.5	2.92	1.52	-0.58	-1.98	50	10.2	9.28	3.59	-0.92	-6.61
26	3.85	2.60	1.17	-1.25	-2.68	51	14.5	13.05	3.84	-1.45	-10.66

4. Conclusions

In the present study, deterministic and geostatistical methods were used to obtain optimal solution for locating groundwater level monitoring networks. Groundwater level maps were created using these two methods and it was compared separately on the basis of measured and predicted values and its associated error differences. It was found that error variances estimated between measured and predicted values were less for geostatistical (ordinary kriging) method and relatively these error variances are much higher for deterministic (IDW) method. Based upon the less error variances it can be concluded that more accurate solutions can be obtained using geostatistical method. In geostatistical method ordinary kriging technique was used to create groundwater level map. Standard error map created using ordinary kriging interpolation method with regions having minimum and maximum error variances is shown in Figure 6. Location having maximum standard errors can be considered for optimal deign of observation networks of wells. From standard error map, it was found that maximum error variances is observed in central and

north eastern part of the study area. The density of wells in these areas are also less and therefore these location can be selected for installing additional observation wells. But for selecting site for additional number of wells for groundwater level monitoring, detailed study of local conditions and hydrogeological parameters must also be taken into consideration.

5. References

- *Ahmadi, S., and Sedghamiz, A. (2007). Geostatistical analysis of spatial and temporal variations of groundwater level. Environmental Monitoring and Assessment, 129(1), 277–294.*
- *ASCE.(2003). Long-term Groundwater Monitoring, the State of the Art. Reston, Virginia: USA Task Committee on the State of the Art in Long-Term Ground Water Monitoring Design.*
- *Caers, J. (2005). Petroleum geostatistics. Richardson, Houston: Society of Petroleum Engineers.*
- *Goovaerts, P. (1997). Geostatistics for natural resources evaluation. New York: Oxford University Press.*
- *Jousma, G., Roelofsen, F.J.(2004). World-wide Inventory on Groundwater Monitoring.TNO, Utrecht, The Netherlands: International Groundwater Resources Assessment Centre.*
- *Prakash, M. R., and Singh, V. S. (2000). Network design for groundwater monitoring–A case study. Environmental Geology, 39(6), 628–632.*
- *Shepard, D. (1968). A Two-Dimensional Interpolation Function for Irregularly Spaced Data, Proc.*
- *23rd Nat. Conf. ACM,517–523.*
- *Theodossiou, N., and Latinopoulos, P. (2006). Evaluation and optimisation of groundwater observation networks using the kriging methodology. Environmental Modeling and Software, 21(7), 991–1000.*
- *UNESCO.(1998). Monitoring for Groundwater Management in (Semi-)arid Regions. Paris, France: UNESCO.*
- *Varouchakis, E. A., and Hristopulos D. T. (2013). Comparison of stochastic and deterministic methods for mapping groundwater level spatial variability in sparsely monitored basins Environmental Monitoring Assessment185,1–19.*
- *Vieux, B.E.(2001). Distributed Hydrologic Modeling using GIS,. Kluwer Academic Publishers, Dordrecht: Water Science and Technology Library.*
- *WMO.(1989). Management of groundwater observation programmes. Geneva, Switzerland: Operational Hydrology Report No. 31:WMO.*
- *Zhou, Y., Dianwei, D., Jiurong, L., & Wenpeng, L. (2013). Upgrading a regional groundwater level monitoring network for Beijing Plain, China. Geoscience Frontiers, 4, 127-138.*

Stability Analysis of Submerged Reef Using Soft Computing Techniques

Geetha Kuntoji[1], Subba Rao[2] and Manu[3]

[1]*Research Scholar, Department of Applied Mechanics and Hydraulics, National Institute of Technology Karnataka, Surathkal – 575 025 India,*

[2] *Professor, Department of Applied Mechanics and Hydraulics, National Institute of Technology Karnataka, Surathkal – 575 025 India,*

[3]*Assistant Professor, Department of Applied Mechanics and Hydraulics, National Institute of Technology Karnataka, Surathkal – 575 025 India,*

Email: geeta.kuntoji@gmail.com, *surakrec@gmail.com, manunitk77@gmail.com*

Telephone/Mobile No.: +91 720485805, +91 9448911304, +91 9844087664

ABSTRACT

Breakwaters are widely constructed for the purpose of protecting vital installations on the coast and offshore, for shoreline stabilization and to prevent the siltation of river mouths. We can say that development of breakwater construction is closely related to developments of ports around the world over centuries. Physical model studies of structures such as breakwaters, submerged reef etc, consumes more of time, man power and is expensive. Many experimental works have been carried out on different types of breakwaters by various authors to study their performance which is time consuming and expensive. The prediction by numerical models is not matching with experimental or in- situ data because of complexity and non-linearity associated with it. Hence it is decided to apply soft computing techniques on performance of submerged reef. In the present study the experimental data for submerged reef are collected from Marine Structures Laboratory, Department of Applied Mechanics and Hydraulics, NITK, Surathkal, India. Adaptive Neuro Fuzzy Inference system (ANFIS) model is constructed using experimental data sets to predict the effect of structure and wave characteristics on the hydraulic performance of the reef. The experimental data are used to train ANFIS models and results are determined in terms of statistical measures such as mean square error, root mean square error, correlation coefficient. The result shows that ANFIS can be efficient tools in predicting the performance of wave and structural parameters.

Keywords: Submerged Reef, Stability and Soft-Computing Techniques.

1. Introduction

The environmental impact on the coastal zone is growing rapidly and has led to development of many protective structures for its protection against most destructive forces of the ocean waves and its actions. Even though lot of research is in progress, this is taking different and interesting turns and becoming the ever growing challenge to the coastal engineers to protect the coastal zone with different solutions for different problems encountered as the ocean never shows the similar pattern of wave characteristics.

The above discussion has led to the construction of protective structures such as seawalls, revetments, groins, coral reefs and offshore breakwaters. The function of these structures is to protect beaches, bluffs, dunes and harbour areas from destructive wave action and to maintain the tranquillity condition within the port as well as harbour area by providing protection from dynamic forces of ocean.

Breakwaters are widely constructed for the purpose of protecting vital installations on the coast and offshore, for shoreline stabilization and to prevent the siltation of river mouths. We can say that development of breakwater construction is closely related to developments of ports around the world over centuries. Experimental works have been carried out on different types of breakwaters by Johnson et al. (1951), Brunn P. et al. (1976), Pilarczyk and Ziedler (1996,2003), Neelamani and Sunderavadivelu (2003), Yong-Sik Cho et al. (2003), Shirlal et al. (2005), Cho et al. (2007), Subba Rao et al. (2004, 2008) which is time consuming and expensive.

In physical modelling, there are number of uncertainties associated with many of the governing variables and their effects on performance of breakwater. Hence, in order to overcome the uncertainties involved in physical modelling, soft computing techniques such as Artificial neural networks (ANNs) Mandal et. al., (2007) and Balas et. al., (2010), Fuzzy systems (FS), Genetic algorithm m (GA), Support vector machines (SVM) Harish et. al., (2012) and hybrid of these models like Adaptive Neuro Fuzzy Inference System (ANFIS) are used. Dursun et.al. (2012) carried out estimated discharge capacity of semi-elliptical side weirs by using Adaptive-Neuro Fuzzy Inference System (ANFIS). They used 675 laboratory test results for determining discharge coefficient of semi-elliptical labyrinth side weirs. From their study, ANFIS technique could be successfully employed in modeling discharge coefficient. Patil et al., (2011) and Mase et.al, (1995), have applied ANFIS to solve a wide variety of coastal engineering problems. In practical soft computing techniques are widely used in different fields and accepted as an alternative way to tackle complex problems. Which have an ability to learn from examples and have a capacity to handle noisy and incomplete data to deal non-linear problems. Once model learns from examples then predictions of the outcome can be done at higher rates.

The present paper, deals with the application of the hybrid model ANFIS for predicting the transmission coefficient (K_t) of submerged reef. Comparison of K_t Values obtained in the laboratory experiments and predicted by ANFIS model.

1.1 Submerged Reef

A submerged structure is a kind of offshore structure, with its crest at or below the sea water level. Cross section of the submerged breakwater is generally assumed as a trapezoidal shape as showed in Figure 1.

To study the functions of submerged breakwater, there has been a great deal of contributions from both theoretical and experimental investigations conducted by various investigators with plethora of ideas. According to Johnson et al. (1951), most of them deal with the effects of height, slope, crest width, location etc. of the submerged breakwater on the transformation of wave passing over it. Submerged breakwaters have been effectively used to protect harbour entrances, to reduce siltation in entrance channels, for protection against beach erosion, for creation of artificial fishing grounds and for the protection of coastal structures from damage caused by wave action (Dattatri et al., 1978). According to them, submerged breakwater can affect substantial wave attenuation and can successfully be used in place where tidal variations are small and only partial protection from wave action is required. The important parameters that influence its performance are crest width and crest height of the breakwater. As crest elevation approached the SWL, there is general decrease in transmission coefficient (Dattatri et al., 1978). The best morphological effects are pronounced as accretion of sediment between the submerged breakwater and shoreline and low reflection have been reached for the breakwaters with a slope of the seaward face ranging from 1V : 2H to 1V : 3H (Pilarczyk and Ziedler, 1996).

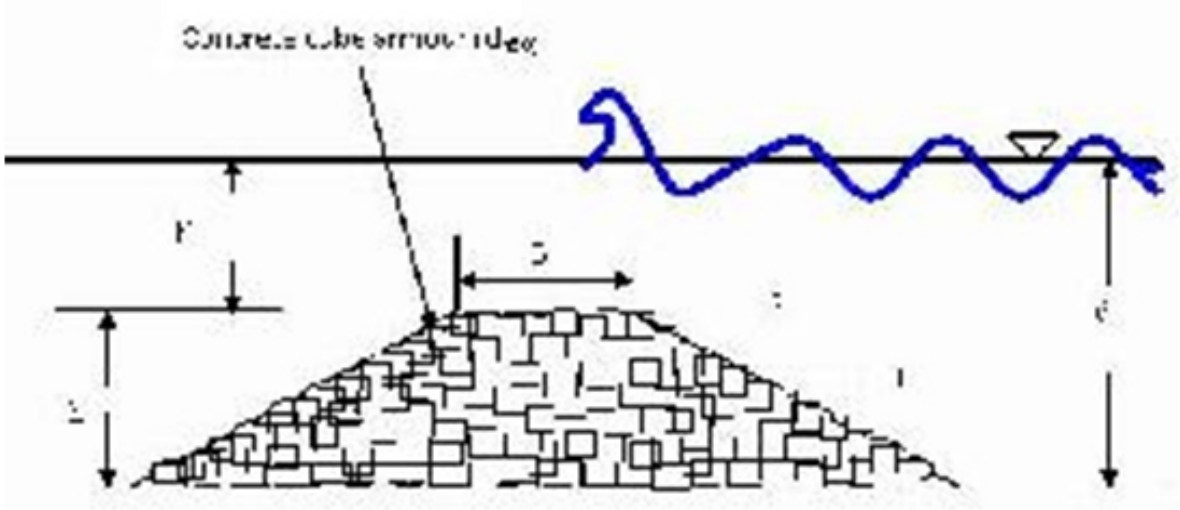

Figure 1 Details of test model of submerged reef

2. Experimental Data

The experimental work was carried in Marine Structures Laboratory, Department of Applied Mechanics and Hydraulics, NITK, Surathkal, India. The wave flume is 50 m long, 0.71 m wide, 1.1 m deep, and has a 42 m long smooth concrete bed. With existing facilities of two dimensional wave flume, regular waves of heights ranging from 0.08 m to 0.24 m and period ranging from 0.8 sec to 4.0 sec can be produced in the range of water depth of 0.25 m to 0.5 m. keeping this in focus, a model scale of 1:30 is selected for the present experimental investigation as shown in Figure 2 and Table 1.

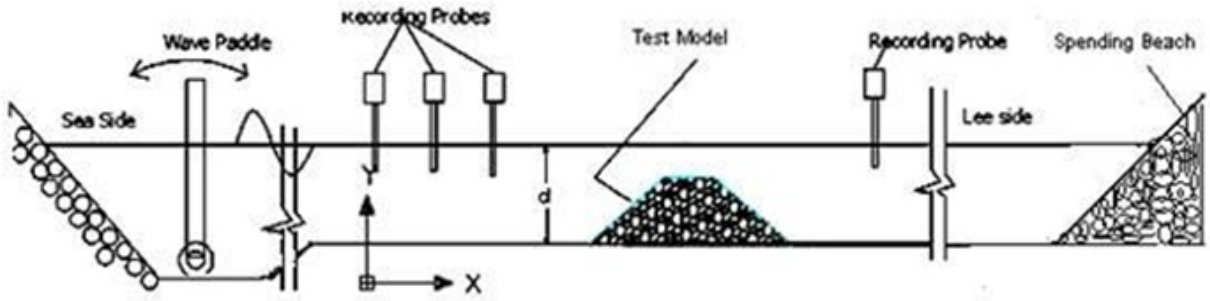

Figure 2 Details of experimental setup

For the present analysis, experimental data are converted into non dimensional parameters like Wave Steepness (H_o/gT^2), relative spacing of reef (X/d), armour stability (h_c/h) and transmitted wave height (H_t) and initial free board (F/H_i) are used for the analysis. 198 data sets are considered for the present study. From 198 data sets randomly 160 (75%) data sets are used for training the networks and 38 (25%) data sets are used for testing the models

Table 1 Range of parameters for experiments

Variable		Experiment Values
Slope	--	1V: 2H
Armour type	--	Concrete cube
Nominal size armour cube	Dn_{50}	0.0255, 0.0244, 0.0232, 0.0218 and 0.0203 m
Armour cube weight	W_{50}	20gm, 25gm, 30gm, 35gm and 40gm
Crest height	h	0.25 m
Crest width	B	0.10 m

3. Adaptive Neuro Fuzzy Inference System

The Adaptive Neuro Fuzzy Inference System (ANFIS) was first introduced by Jang (1993). It is a combination of least-squares and backpropagation gradient decent methods used for training Takagi-Sugeno type fuzzy inference system which is used for an effective search for the optimal parameters. It can provide a starting point for constructing a set of fuzzy 'if-then' rules with appropriate membership functions to generate the fixed input-output pairs. The advantage of a hybrid approach is that it converges much faster, since it reduces the search space dimensions of the backpropagation method used in neural networks.

3.1 Architecture of ANFIS

A simple architecture of ANFIS with I-input variables namely $i_1=H_o/gT^2$, $i_2=F/H_i$, $i_3=H_t$, $i_4=h_c/h$, $i_5= X/d$ and o is output variable i.e., o=transmission coefficient (K_t) It consists of five layers and each layer is explained below.

Layer 1

Every node in this layer is an adaptive node with a node function

$$O_{1,i}=\mu A_i(x), \quad \text{for } i=1,2 \tag{3.1}$$

$$O_{1,i}=\mu B_{i-2}(x), \quad \text{for } i=3,4 \tag{3.2}$$

x (or y) is the input node and A_i (or B_{i-2}) is a linguistic variables associated with the membership function of a fuzzy set (A_1,A_2,B_1,B_2).Typical membership function:

$$\mu A(x)=\frac{1}{1+\left[\frac{c_i}{a_i}\right]^{2b_i}} \tag{3.3}$$

Where a_i, b_i and c_i is the parameter set. Parameters are called as premise parameters.

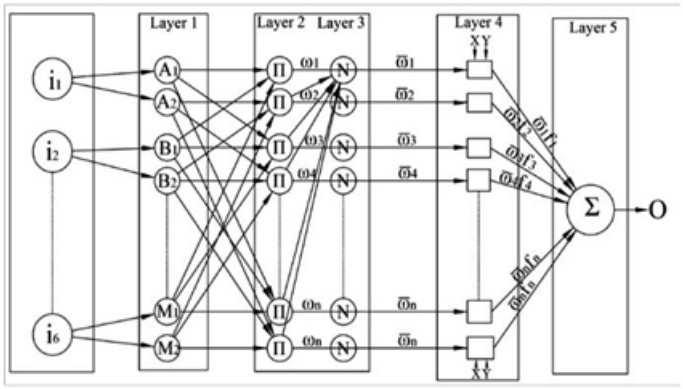

Figure 3 ANFIS structure

Layer 2

Each node in this layer is a fixed node, indicated by Π Norm. The output is the product of all the incoming signals.

$$O_{2,i}=w_i=\mu A_i(x)\cdot\mu B_i(y), \quad i=1,2 \tag{3.4}$$

Output signal w_i represents the fire strength of a rule.

Layer 3

Each node in this layer is a fixed node N Norm. The i^{th} node calculates the ratio of the firing strength to the sum of the firing strength:

$$O_{3,i}=\bar{w}_i=\frac{w_i}{w_1+w_2}, \quad i=1,2 \tag{3.5}$$

Output signal $\overline{w}_i$ is called normalized firing strengths.

Layer 4

Each node in this layer is an adaptive node, indicated by square node with a node function:

$$O_{4,i}=w_i f_i=w_i(p_i x+q_i y+r_i) \quad (3.6)$$

where w_i is the normalized firing strength from layer 3. $\{p_i, q_i, r_i\}$ is the parameter set which are called as consequent parameters.

Layer 5

Each node in this layer is a fixed node, indicated by circle node which computes the overall output as the summation of all incoming signals:

$$\text{Overall output, } S=O_{5,1}=\sum_i \overline{w}_i f_i=\frac{\sum_i w_i f_i}{w_i} \quad (3.7)$$

The different membership functions assigned for input parameters are:
Gauss membership function:

$$f(x,\sigma,c)=e^{\frac{-(x-c)^2}{2\sigma^2}} \quad (3.8)$$

where x is input parameters, c and σ are mean and variance respectively. Triangular membership function:

$$f(x,a,b,c)=\max\left(\min\left(\frac{x-a}{b-a},\frac{c-x}{c-b}\right),0\right) \quad (3.9)$$

where, x is input parameter, a & c locate the feet of the triangle and b locate the peak.
Generalized bell-shaped membership function:

$$f(x,a,b,c)=\frac{1}{1+\left|\frac{x-c}{a}\right|^{2b}} \quad (3.10)$$

where, x is input parameter, c locate the centre of the curve.

4. Results and Discussion:

In the present study, Adaptive Neuro Fuzzy Inference System (ANFIS) is used to predicting the transmission coefficient K_t of submerged reef. The performance of the model is evaluated using statistical measures which are defined as follows:

MeanSquareError

$$(MSE) = \frac{1}{n}\sum_{i=1}^{n}\left|\frac{O_i - P_i}{P_i}\right|^2 \times 100\% \quad (4.1)$$

RootMeanSquareError

$$(RMSE) = \sqrt{\frac{1}{n}\sum_{i=1}^{n}\left(\frac{O_i - P_i}{P_i}\right)^2} \times 100\% \quad (4.2)$$

CorrelationCoefficient

$$(CC) = \frac{\sum_{i=1}^{n} P_i O_i}{\sqrt{\sum_{i=1}^{n} P_i^2 \sum_{i=1}^{n} O_i^2}} \quad (4.3)$$

ScatterIndex

$$(SI) = \frac{\sqrt{1/n\sum_{i=1}^{n}((P_i - \bar{P}_i) - (O_i - \bar{O}_i))^2}}{\bar{O}} \quad (4.4)$$

Where, O and P are observed and predicted transmission coefficient respectively, n is the number of data set used and $\bar{P}\&\bar{O}$ are average predicted and observed transmission coefficient respectively.

ANFIS model is developed to predict the transmission coefficient of submerged reef. Out of 198 experimental data set, 160 data set are used for training the model and 38 data set are used for testing the model. The ANFIS model, with a combination of gradient descent algorithm and least squares algorithm is used for an effective search for the optimal parameters to yield good results. Based on this hybrid approach, correlations of training and testing are increased. Here, Sugeno first order with 64 fuzzy rules and 2 generalized 'gauss' membership functions are used to train the model.

The results obtained during training and testing processes for input parameters are calculated by means of statistical measures like Correlation Coefficient, Mean Square Error, Root Mean Square Error values and Scatter Index are shown in Table 2. MSE and RMSE of Gaussian model are 1.456, 1.14, 8.445, 2.91 and SI is 0.10 and 0.225 for training and testing is less than all other (Triangular and Gbell membership functions) models. Fig.4 and Fig 5 shows the correlation between the observed and predicted transmission coefficient K_t for train and test of ANFIS model with gauss and triangular membership functions respectively.

The ANFIS model with 64 fuzzy rules and 2 generalized gauss membership function is used, which reduces the processing time and gives better results for prediction of K_t. The ANFIS with gauss membership function model outperformed the other ANFIS membership model and provided the best performance, i.e., the lowest RMSE and highest CC for test output. Results of the study also indicate that the predictive capability of the ANFIS with gauss membership function model used in this study is better when compared with other membership function models.

Table 2 Statistical Measures for different Model

Model		Membership Function	MSE	RMSE	CC	SI
ANFIS	Train	Gauss	1.456	1.14	0.99	0.100
	Test		8.445	2.91	0.97	0.225
	Train	Triangular	1.447	1.212	0.86	0.211
	Test		16.45	3.541	0.68	0.427
	Train	Gbell	1.521	1.201	0.97	0.104
	Test		42.01	7.001	0.69	0.602

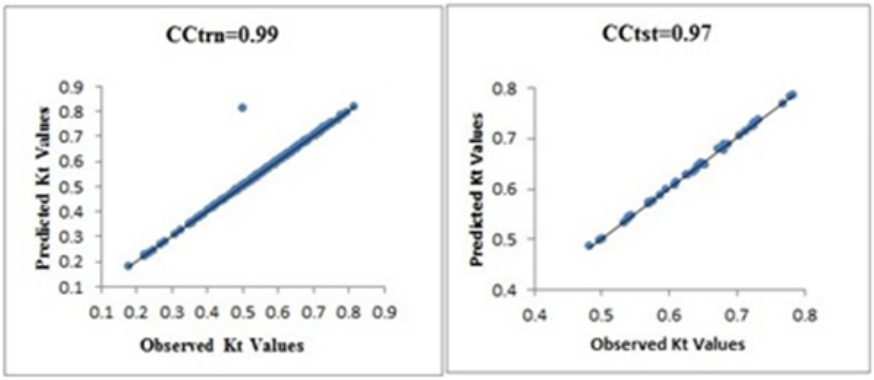

Figure 4 Observed & Predicted K_t values by Anfis using Gauss Membership Function for Train &Test Data, respectively.

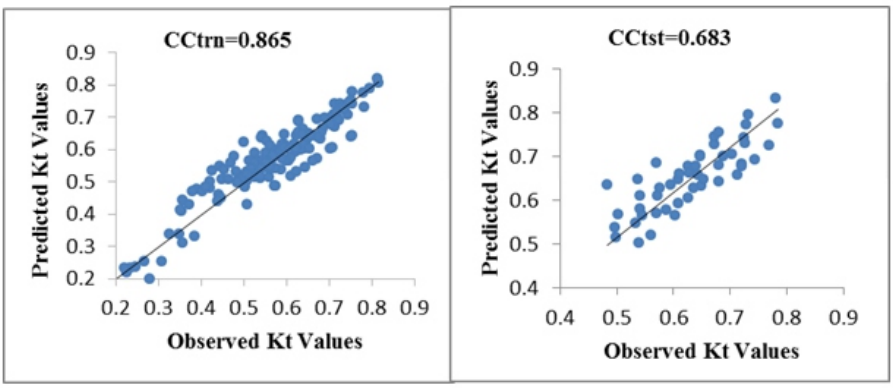

Figure 5 Observed & predicted K_t values by ANFIS using triangular membership function for train & test data respectively.

5. Conclusions

The model shows good results in terms of statistical measures like mean square error, root mean square error, correlation coefficient and scatter index for observed and predicted transmission coefficient Values. ANFIS structure which uses first order Sugeno Containing 64 rules and 2 generalised gauss membership functions yields good results compared to other types of membership functions. The K_t values predicted by ANFIS and obtained in experimental work are nearly equal.

The efficiency of the ANFIS models depends on the number of membership functions associated with each input data. From the present study we can conclude that Soft computing approach reduces time and predicts the transmission coefficient very fast in comparison with the Experimental work. Hence, ANFIS model is an effective tool in predicting the transmission coefficient K_t of
submerged reef very fast and investigate the stability of the submerged reef. Therefore it can be used as an alternative tool to determine the K_t of submerged reef.

References:

Balas C. E., Koc M. L. and Tur R., 2010. Artificial neural networks based on principal component analysis, fuzzy systems and fuzzy neural networks for preliminary design of rubble mound breakwaters. J. Applied Ocean Research, 32, pp.425-433.

Brunn, P. and Johannesson P., 1976. Parameters affecting stability of rubble mound. J. Waterways, Harbors and Coastal Engineering Division, 102, pp.141-163.

Dattatri, J., Raman, H. and Jothi Shankar, N. (1978). "Performance characteristics of submerged breakwater." Proceedings of 16th Coastal Engineering Conference, Hamburg, pp 2153 – 2171.

Dursun, O. F., Kaya, N., & Firat, M. (2012). Estimating discharge coefficient of semi-elliptical side weir using ANFIS. Journal of Hydrology, 426, 55-62.

Earth sciences and Engineering, vol. 05, No. 04 (02), August, 1046-1051.

Harish N., Sukomal Mandal, Subba Rao, and Lokesha, (2012), "Adaptive neuro fuzzy inference system modeling to predict damage level of non-reshaped berm breakwater", International Journal of

Jang J.S.R., 1993. ANFIS: Adaptive Network Fuzzy Inference System. IEEE Transactions on Systems, Man, and Cybernetics 23 (3), pp. 665-685.

Johnson, R. R., Mansard, E. P. D. and Ploeg, J. (1978). "Effect of wave grouping on breakwater stability." Proc. 10th Int. Conf. on Coast. Eng., ASCE, 2228-2247.

Mase H., Masanobu S. and Tetsuo S., 1995. Neural network for stability analysis of rubble mound breakwater. J. of waterway, port, coastal and Ocean Engineering, 121(6), pp.294-299.

Neelamani, S. and Sunderavadivelu, R. (2003). "Plans to win back a sandy beach in Pondicherry,

Park, S. H., Lee, S. O., Jung, T. H. and Cho, Y. S. (2007). "Effects of submerged structure on rubble mound breakwater: Experimental study." KSCE Journal of Civil Engineering, Vol. 11, No.6, pp 277-284.

Patil S.G., Mandal S., Hegde A.V. and Alavandar S., 2011. Neuro-fuzzy based approach for wave transmission prediction of interlaced multilayer moored floating pipe breakwater. J. Ocean Engineering, 38, pp.186-196.

Pilarczyk, K. W. and Zeidler, R. B. (1996). "Offshore breakwater and shore evolution control." A. A. Balkema Rotterdam, Netherlands pp. 572.

Pilarczyk, K.W. (2003), Design of Low-crested (Submerged) Structures -an overview. Proceedings of 6th International Conference on Coastal and Port Engineering in Developing Countries, Colombo, Sri Lanka, 1-18

Shirlal, K. G., (2005). "Studies on the stability of conventional rubble mound breakwater defenced by a submerged reef." PhD Thesis, N. I. T. K., Surathkal, India.

Shirlal, K. G., Rao, S. and Manu (2008). "Performance of a Submerged Reef - A Physical Model

South-East coast of India." Proceedings of the 3rd International Surfing Reef Symposium, June, Raglan, New Zealand, pp 375 – 377.

Study." International Journal of Ecology and Development, Vol. 11, No. F08, Fall 2008, pp 90 - 98.

Subba Rao, Subrahmanya K., Rao B.K., and Chandramohan V. R., 2008. Stability aspects of nonreshaped berm breakwaters with reduced armor weight. J. Waterway, Port, Coastal, and Ocean Engineering, 134, pp.81-87.

Yagci O., Mercan D.E., Cigizoglu H.K. and Kabdasli M.S., 2005. Artificial intelligence methods in breakwater damage ratio estimation. J.Ocean Engineering, 32, pp. 2088-2106.

Optimization of Grid Size And Time Step For Simulation of Flow Through Orifice Spillway

Mrs. Prajakta P. Gadge [1], Prof. V. Jothiprakash[2], Dr. (Mrs.) V. V. Bhosekar[3]

[1]Research Scholar, IIT Bombay, Mumbai-400076, and Scientist B, Central Water and Power Research Station, Pune-411024, India

[2]Professor, IIT Bombay, Mumbai-400076, India

[3] Scientist E, Central Water and Power Research Station, Pune-411024, India

(Corresponding author: prajaktagadge@gmail.com)

ABSTRACT

Computational Fluid Dynamics or CFD is the analysis of system involving fluid flow, heat transfer and associated phenomenon such as chemical reactions by means of computer based simulation. It provides a qualitative and sometimes even quantitative prediction of fluid flows by means of mathematical modeling using partial differential equations, numerical methods and software tools. In the present study, Computational Fluid Dynamic Software FLUENT version 6.3.26 has been used for numerical simulation of flow through orifice spillway. Systematic grid convergence and iterative convergence studies are the primary methods for building and quantifying the confidence between modeling and simulation. The present paper discusses results of grid convergence and iterative convergence of the solution with respect to different hydraulic parameters of an orifice spillway. The numerical model was verified in terms of grid convergence by comparing the results of numerical simulation with the results of physical model for different grid sizes. The numerical model was run till the convergence of the solution is reached with the optimized grid size. Realizable k-ε turbulence model with Modified HRIC scheme was used for numerical simulation. Variation in different hydraulic parameters such as discharge through orifice, pressures on the roof and spillway bottom surface and water surface profiles were studied at different time steps. The results are discussed in detail in the present paper. The data was compared with the physical model and was found in good agreement.

Keywords: Numerical model, physical model, grid size and time step, orifice spillway

1. Introduction

Computational Fluid Dynamics, commonly known by the acronym 'CFD', is a branch of Fluid Mechanics that resolves fluid flow problems numerically. The foundation on which CFD is built is the Navier-Stokes equations, the set of partial differential equations that describe fluid flow. With CFD, the area of interest is subdivided into a large number of cells or control volumes. In each of these cells, the Navier-Stokes partial differential equations can be rewritten as algebraic equations that relate the velocity, temperature and pressure. The resulting set of equations can then be solved iteratively, yielding a complete description of the flow throughout the domain. By solving the fundamental equations governing fluid flow processes, CFD provides information on important flow characteristics such as pressure loss, flow distribution and mixing rates.

There are number of commercially available powerful CFD software such as FLUENT, FLOW-3D, Star CD etc. which are being used by the researchers for simulating the flow over the spillway. Cheng Xiangju et al. (2006) studied the numerical simulation of air -water two phase flows over stepped spillways using FLUENT software. P.G. Panel et al. (2007) discussed three dimensional numerical modelling of several different spillway configurations using CFD software FLOW 3D. Dargahi B. (2006) carried out experimental study and 3D numerical simulations using CFD code FLUENT for a free-overflow spillway. Bhosekar (2011) provided guidelines for hydraulic design of aerator on orifice spillway based on both physical and numerical model studies. Jothiprakash et al. (2015) used FLUENT software to study the air water flow characteristics of orifice spillway using numerical model studies.

CFD simulation includes various steps such as formulation of the flow problem, modelling the geometry and flow domain, defining boundary and initial conditions, generation of grid, establishing the simulation strategy, creating the input parameters and files, performing the simulation, monitoring the simulation for completion, post-processing to get the results, comparing the results, repeating the process to examine sensitivity. Each step in CFD simulation has its own importance. The grid convergence and iterative convergence are two important processes in CFD simulation for getting accurate results. There are no universal metrics for judging convergence. The spacing of the grid points determines the local error and hence the accuracy of the solution. Spacing also determines the number of calculations to be made to cover the domain of the problem and thus the cost of the computation. In the present study, Computational fluid dynamic software FLUENT version 6.3.26 has been used for numerical simulation of flow through orifice spillway. The numerical model was verified in terms of grid convergence and iterative convergence by comparing the results with results of physical model.

2. Physical and Numerical Model Set Up

The physical model was constructed at Central Water and Power research Station (CWPRS), Pune to a scale of 1:50 based on Froude number criteria. The model was constructed in 15 mm transparent Perspex sheet to visualize the flow conditions throughout the length of the spillway. Necessary arrangements were made for measurement of discharge, pressures on roof profile and spillway bottom surface and water surface profiles along the centre line of spillway. Figure 1 and 2 shows the side view and cross section of physical model.

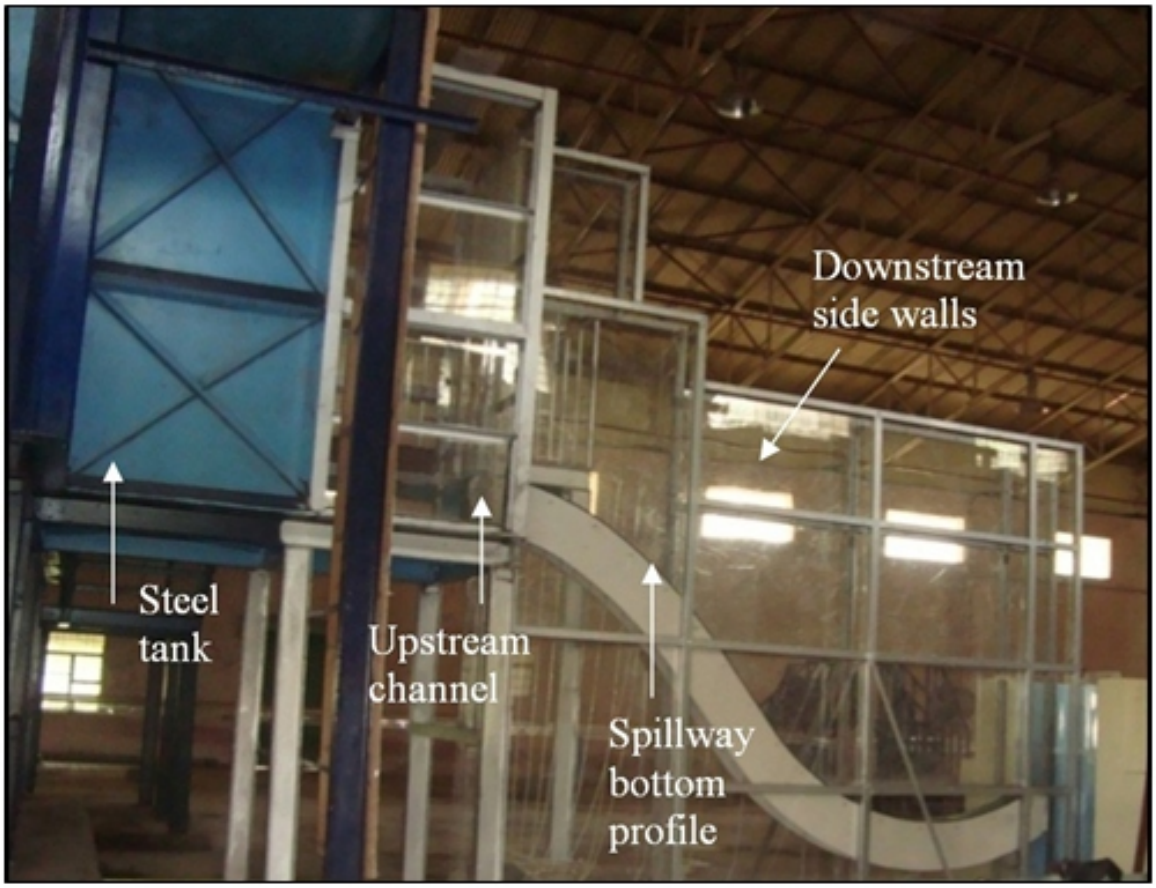

Figure 1: Side View of the physical model

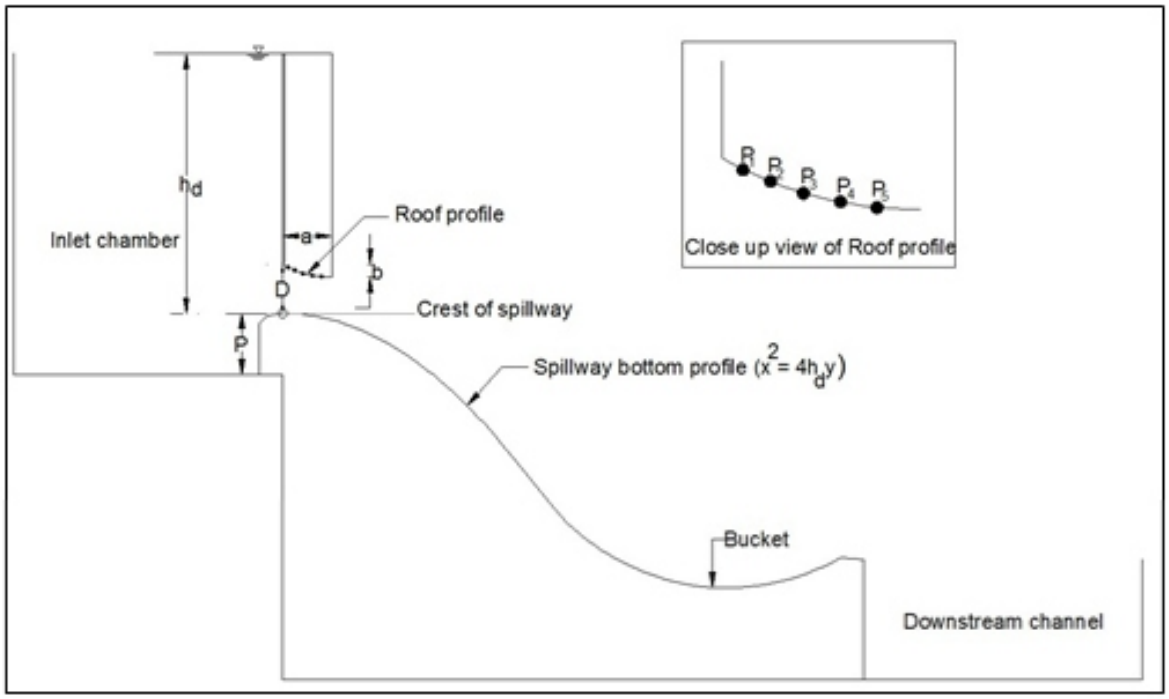

Figure 2: Cross section of spillway

Experiments were conducted on a spillway bottom profile designed for a head of 0.8 m. The orifice size was selected as 0.2 m x 0.28 m for the study. The head over the crest was 0.8 m.

Numerical simulations were carried out for the same configurations of design head and orifice size studied in physical model. The domain of the problem consisted of inlet channel with piers and upstream spillway curve, spillway channel with the roof profile of the orifice spillway and downstream channel. Geometry of 3-D orifice spillway model was prepared in Gambit software. Hexahedral cells were used throughout the domain. In the present paper, the main aim is to optimize the grid size for modeling the orifice type of flows. In view of this, five different sizes of grids i.e. 0.004 m, 0.008 m, 0.012 m, 0.024 m and 0.05 m were used for numerical simulation. These grid sizes were used throughout the width of the spillway. Coarser mesh was generated in other regions of less interest. Air was selected as primary phase and water as secondary phase. Pressure inlet boundary condition was defined at domain inlet. All the air boundaries were defined as pressure inlet boundaries on which atmospheric pressure was assumed. The outlet of domain was defined as pressure outlet boundary, so that water can flow out freely. All the walls were set as the stationary, non-slip wall. Figure 3 shows grid generation and boundary condition of the entire domain.

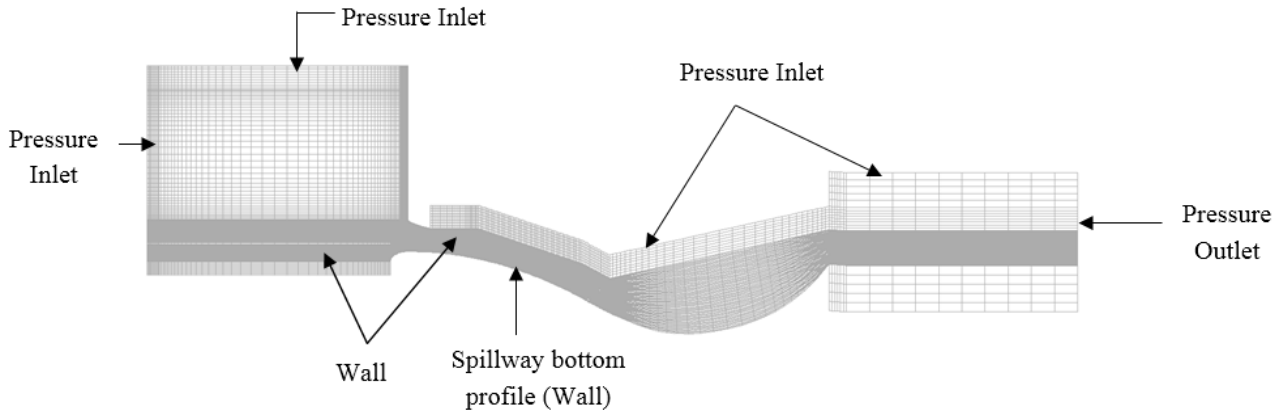

Figure 3: Grid Generation and boundary condition of the domain

Realizable k-ε turbulence model with modified HRIC scheme was used for numerical simulation. Numerical model was run with initial time step of 0.001 sec and continued till the convergence was reached. Figure 4 shows the convergence plot for the volume flow rate at orifice opening.

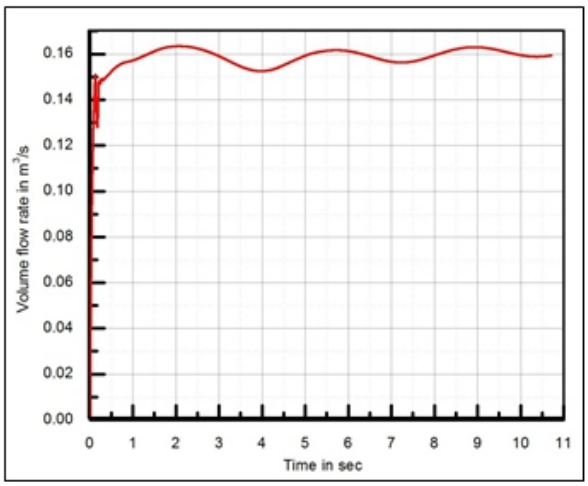

Figure 4: Convergence plot for volume flow rate at orifice opening

It can be seen from the Figure 4 that the solution reached the convergence state after 8 sec in term of volume flow rate at orifice opening. Once the convergence was reached, the numerical model data was extracted and post processing was carried out.

3. Results and Discussions

The results in term of discharge at orifice opening, pressures on roof and bottom profile of orifice spillway and water surface profile along the centerline of spillway computed from numerical model were compared with the results of physical model. The results in term of grid convergence and iterative convergence are discussed below.

Grid convergence

Initially the results were compared for different sizes of grid. Table 1 shows the comparison of discharge through orifice opening between physical and numerical model.

Table 1 Variation in discharge through orifice at different grid size

Grid size in m	Discharge in m^3/s	
	Numerical model	Physical model
0.004	0.163	0.169
0.008	0.164	
0.012	0.159	
0.024	0.159	
0.05	0.158	

Table 1 shows that the discharge through orifice estimated in physical model was closer to the discharge computed in numerical model for fine grid size. There was a difference in discharge for coarser mesh.

Figures 5, 6 and 7 show the comparison of pressures on roof profile, spillway bottom surface and water surface profile respectively between physical model and the results obtained from the numerical model with different grid sizes.

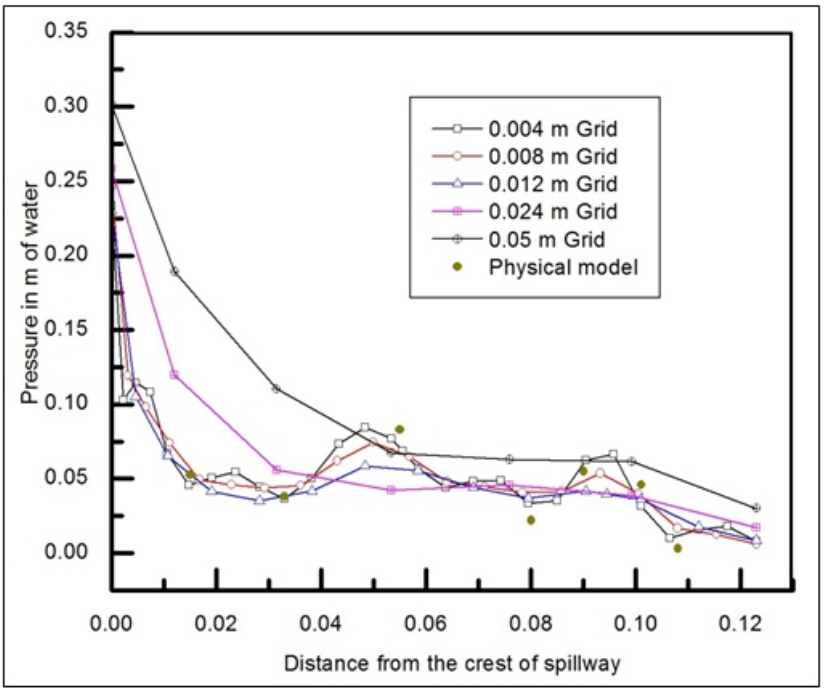

Figure 5: Variation in pressure on roof profile with respect to grid sizes

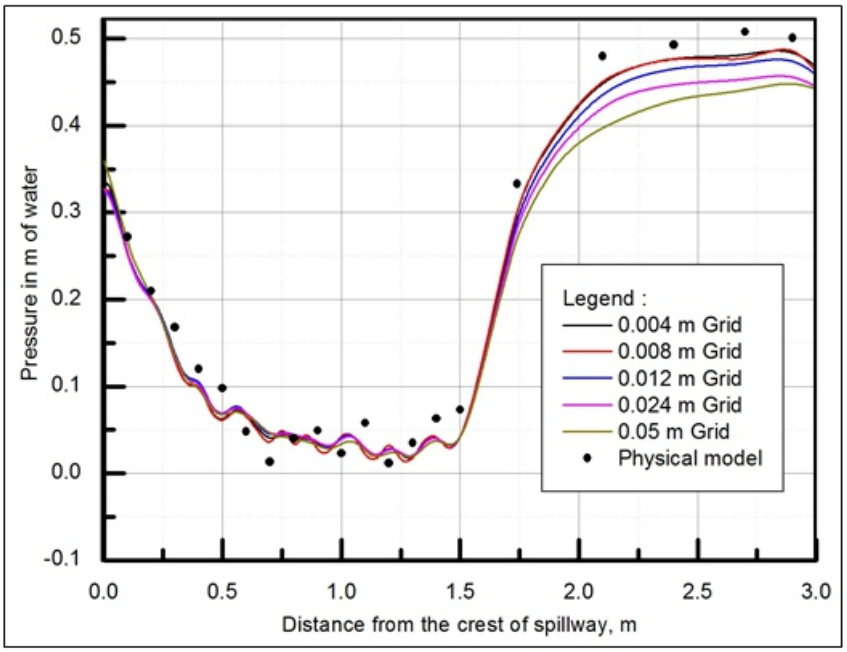

Figure 6: Variation in pressure on spillway bottom profile with respect to grid sizes

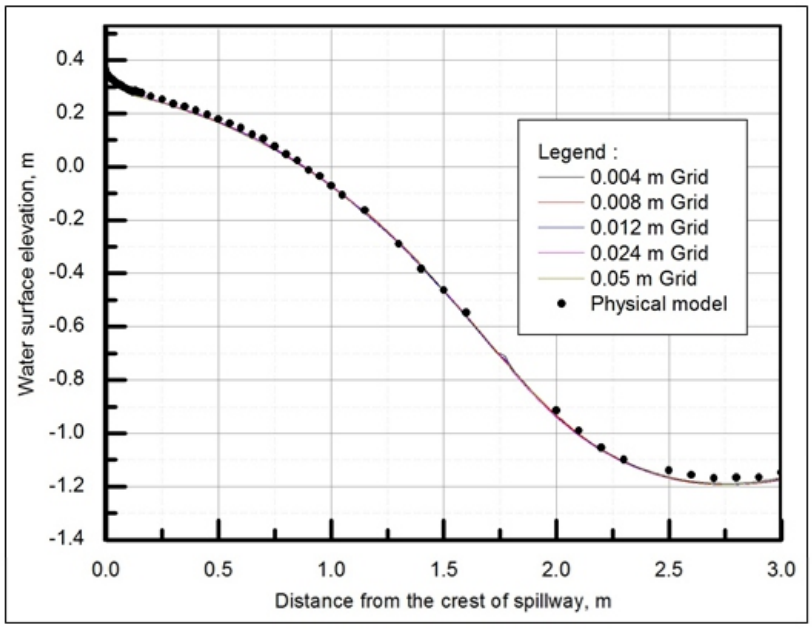

Figure 7: Variation in water surface profile along centerline of spillway with respect to grid sizes

Figure 5 indicates a large variation in pressures obtained in physical model and numerical model with grid size of 0.024 m and 0.05 m. However, the pressure profile computed in numerical simulation with grid size of 0.004 m was closer to the profile obtained in physical model. It can been seen from Figure 6 that there is a fluctuation in pressure up to a distance of 1.5 m. Beyond that distance, the pressure is getting closer to the physical model results with grid size 0.004 m. It is observed that the water surface profiles computed for different grid sizes were coinciding and matching with the results of physical model studies. Flow conditions along the spillway profile were also observed for different grid sizes. Figure 8 shows flow condition along the spillway profile for grid size of 0.004 m. It was observed that the flow conditions were smooth throughout the length of spillway.

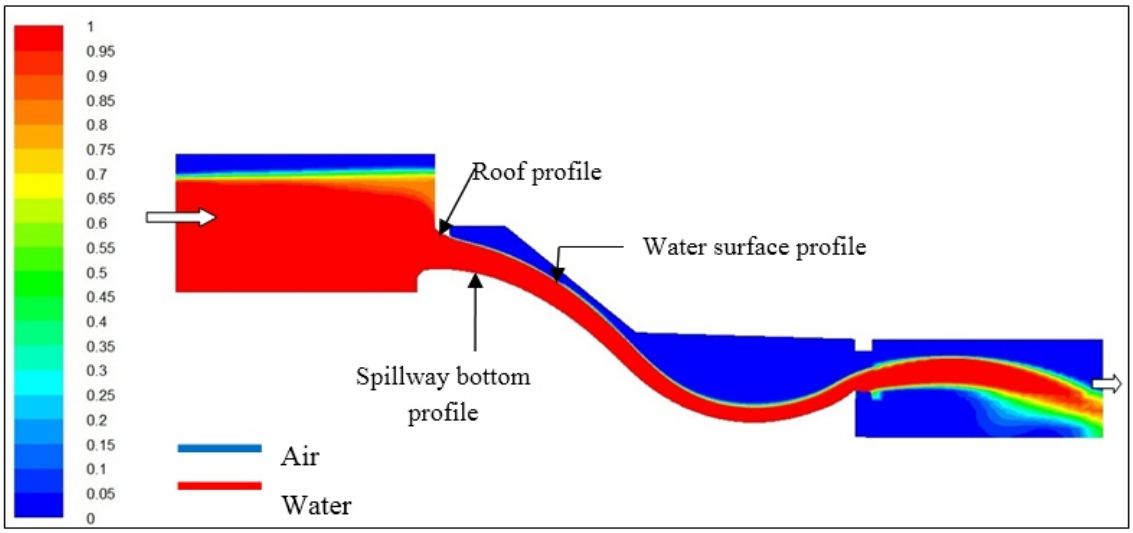

Figure 8: Flow condition along spillway profile for grid size of 0.004 m

Based on the above observations, the grid size of 0.004 m was optimized for modeling the flow through orifice spillway.

Iterative convergence

The numerical simulation run with grid size of 0.004 m was selected and the variation in discharge, pressures and water surface profile was studied for different time steps. Table 2 shows the variation in discharge for different time steps and comparison with results of physical model studies.

Table 2 Variation in discharge through orifice for different time steps

Time in Sec	Discharge in m^3/s	
	Numerical model	Physical model
1.5 sec	0.159	0.169
2.5 sec	0.162	
3.5 sec	0.154	
4.5 sec	0.154	
5.3 sec	0.160	
8.8 sec	0.162	
9.8 sec	0.160	
10 sec	0.163	

The comparison in the table 2 shows that there is a large variation in discharge value up to 4.5 sec. However, the discharge through orifice stabilizes after 5.3 sec and is closer to the discharge value obtained in physical model.

Figures 9, 10 and 11 show the comparison of pressures on roof profile, pressures on spillway bottom surface and water surface profile respectively between physical model and the results obtained from the numerical simulation at different time steps.

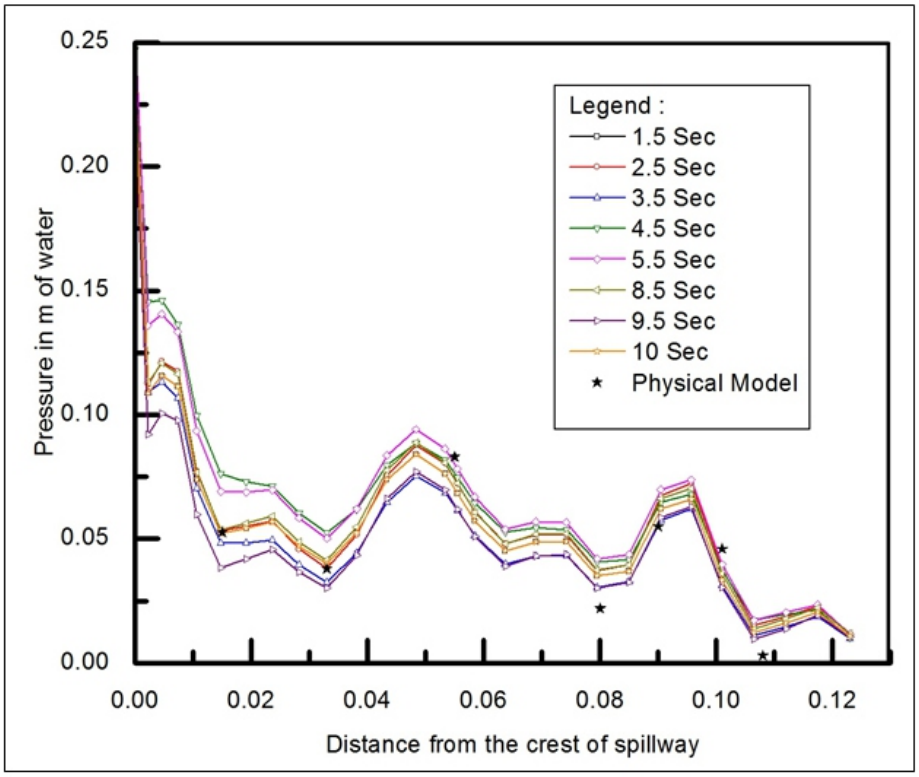

Figure 9: Variation in pressures on roof profile at different time steps

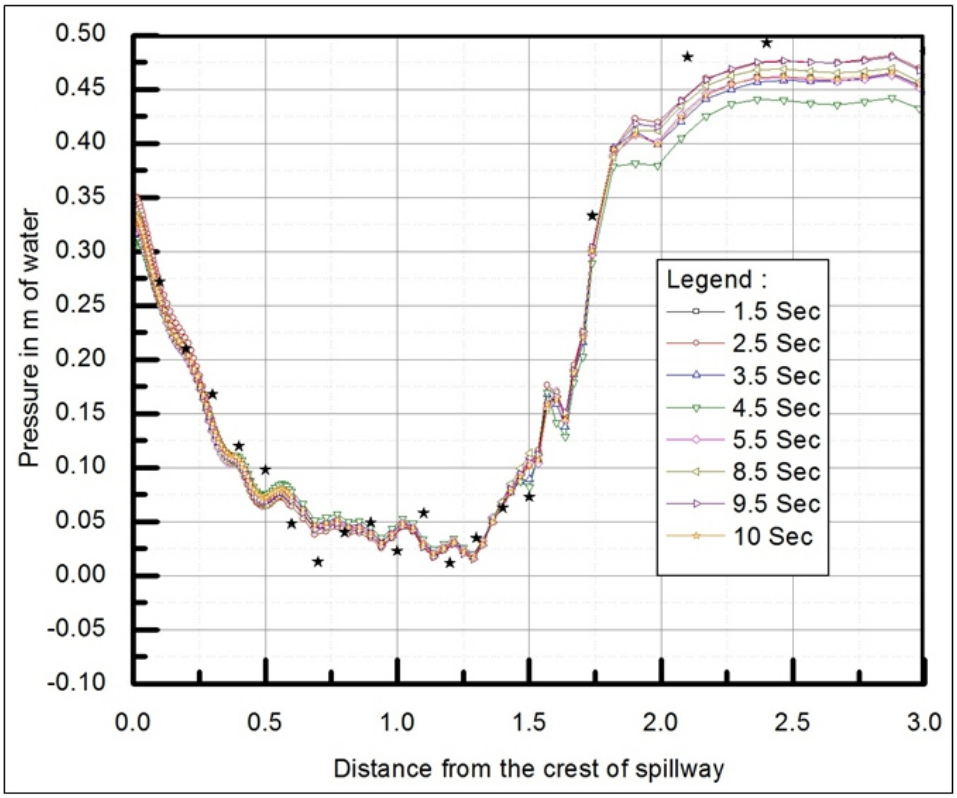

Figure 10: Variation in pressures on spillway bottom profile at different time steps

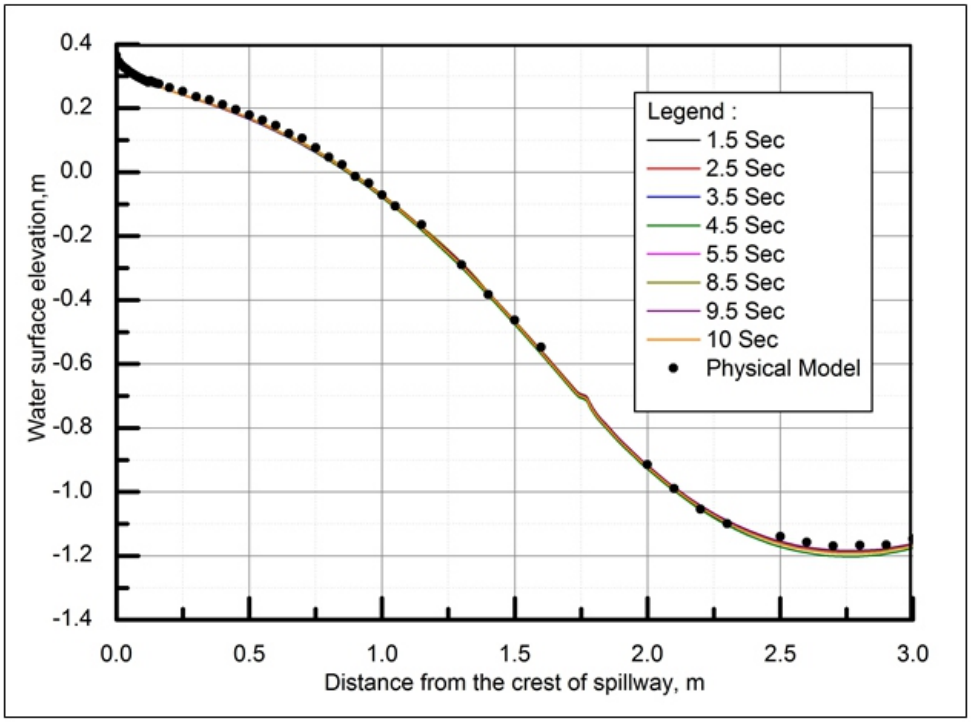

Figure11: Variation in water surface profile along centerline of spillway at different time steps

Figure 9 shows that there is a large fluctuation in the pressures on the roof profile at different time steps. When flow passes through orifice it changes from subcritical to supercritical state with a very high velocity. Due to the continuous fluctuating phenomena, pressures on the roof profile do not remain constant in both physical and numerical model. Hence there is a difference in the values obtained from physical and numerical model studies. Figure 10 shows that there is small variation in pressures on spillway bottom profile up to the distance of 1.75 m. After this, there are fluctuations in pressures values. Beyond 1.75 m, the flow enters into the bucket causing increase in pressure and reduction in velocity. Due to this transition of flow, there is unstable pressure distribution in the bucket portion. Hence, it is very difficult to optimize the time step for such unstable phenomena. It was observed that there was a minor change in water surface profile obtained at every time step as shown in Figure 11. The water surface profile computed in numerical model was matched with the profile obtained in physical model.

In addition to the above studies, five probes were also selected on the roof profile (location as seen in figure 2) to see the variation in pressure with respect to time. The pressure was recorded at different time step and plotted as shown in Figure 12.

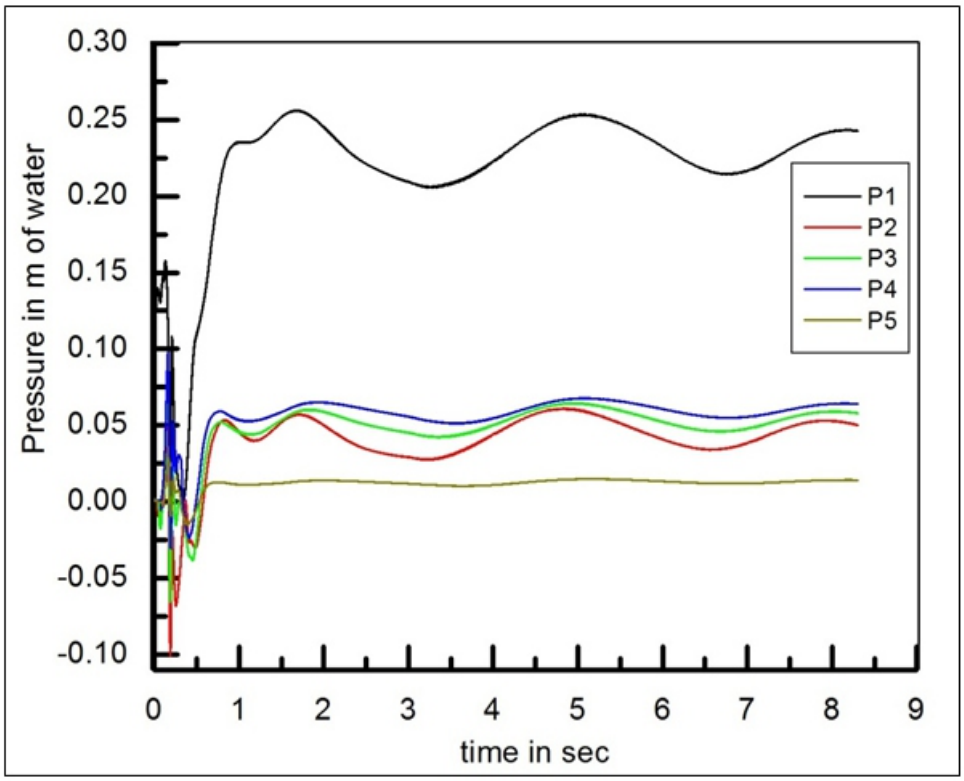

Figure12: Variation in pressure on roof profile of spillway with respect to time

It is seen from Figure 12 that there is a large fluctuation in pressure at P1which was fixed on the roof profile near entrance of orifice due to a sudden transition from subcritical to supercritical flow at the orifice entrance. The pressures were stable at probe P6 which is fixed at the end of roof profile.

4.0 Conclusions

Numerical model used in the present study is verified and validated in terms of grid convergence and iterative convergence. Results of numerical simulation with different sizes of grid were compared with the results of physical model studies in terms of discharge through orifice, pressures on roof and spillway bottom surface and water surface profile along the centerline of spillway. Based on the comparison of results, the grid size of 0.004 m was optimized for modeling the flow through orifice spillway. The variation in the hydraulic parameters was also studied at different time steps. Results of physical model studies were compared with the numerical model in every hydraulic aspect and were found in good agreement. Thus, CFD can be used as a complementary tool along with physical model studies for modeling the flow through orifice spillway.

ACKNOWLEDGMENTS

The first and third authors are grateful to Shri S. Govindan, Director, CWPRS for the consent to publish this paper and provide the facility to conduct physical model studies in CWPRS.

References

Bhosekar V.V. (2011). Physical and Numerical Model Studies for Aerator on Orifice Spillway. Ph.D. Thesis, Indian Institute of Technology Bombay, Mumbai.

Cheng X., Chen Yongcan, Luo Lin. (2006). Numerical simulation of air-water two-phase flow over stepped spillway. Science in China series E: Technological science, 49(6), 674-684.

Dargahi B. (2006), Experimental Study and 3-D Numerical Simulations for a Free-Overflow Spillway. Journal of Hydraulic Engineering, ASCE 132(9),899-907.

FLUENT (2006) Version 6.3.26. Documentation Manual and User's guide.

Jothiprakash, V., Bhosekar, V.V., Deolalikar, P. B. (2015). Flow characteristics of orifice spillway aerator: Numerical model studies. ISH Journal of hydraulic engineering, 21(2), 216-230

Panel, P. G., and Doering, J. C. (2007). An Evaluation of the Computational Fluid Dynamics for Spillway Modeling. 16th Australian Fluid Mechanics Conference, 1201-1206.

Versteeg, H. K., and Malalasekera, W. (1995). An Introduction to Computational Fluid Dynamics-The Finite Volume Method. Longmaon Scientic & Technical, England.

Instructions for Authors

Essentials for Publishing in this Journal

1 Submitted articles should not have been previously published or be currently under consideration for publication elsewhere.

2 Conference papers may only be submitted if the paper has been completely re-written (taken to mean more than 50%) and the author has cleared any necessary permission with the copyright owner if it has been previously copyrighted.

3 All our articles are refereed through a double-blind process.

4 All authors must declare they have read and agreed to the content of the submitted article and must sign a declaration correspond to the originality of the article.

Submission Process

All articles for this journal must be submitted using our online submissions system. http://enrichedpub.com/ . Please use the Submit Your Article link in the Author Service area.

Manuscript Guidelines

The instructions to authors about the article preparation for publication in the Manuscripts are submitted online, through the e-Ur (Electronic editing) system, developed by **Enriched Publications Pvt. Ltd**. The article should contain the abstract with keywords, introduction, body, conclusion, references and the summary in English language (without heading and subheading enumeration). The article length should not exceed 16 pages of A4 paper format.

Title

The title should be informative. It is in both Journal's and author's best interest to use terms suitable. For indexing and word search. If there are no such terms in the title, the author is strongly advised to add a subtitle. The title should be given in English as well. The titles precede the abstract and the summary in an appropriate language.

Letterhead Title

The letterhead title is given at a top of each page for easier identification of article copies in an Electronic form in particular. It contains the author's surname and first name initial .article title, journal title and collation (year, volume, and issue, first and last page). The journal and article titles can be given in a shortened form.

Author's Name

Full name(s) of author(s) should be used. It is advisable to give the middle initial. Names are given in their original form.

Contact Details

The postal address or the e-mail address of the author (usually of the first one if there are more Authors) is given in the footnote at the bottom of the first page.

Type of Articles

Classification of articles is a duty of the editorial staff and is of special importance. Referees and the members of the editorial staff, or section editors, can propose a category, but the editor-in-chief has the sole responsibility for their classification. Journal articles are classified as follows:

Scientific articles:

1. Original scientific paper (giving the previously unpublished results of the author's own research based on management methods).

2. Survey paper (giving an original, detailed and critical view of a research problem or an area to which the author has made a contribution visible through his self-citation);

3. Short or preliminary communication (original management paper of full format but of a smaller extent or of a preliminary character);

4. Scientific critique or forum (discussion on a particular scientific topic, based exclusively on management argumentation) and commentaries. Exceptionally, in particular areas, a scientific paper in the Journal can be in a form of a monograph or a critical edition of scientific data (historical, archival, lexicographic, bibliographic, data survey, etc.) which were unknown or hardly accessible for scientific research.

Professional articles:

1. Professional paper (contribution offering experience useful for improvement of professional practice but not necessarily based on scientific methods);
2. Informative contribution (editorial, commentary, etc.);
3. Review (of a book, software, case study, scientific event, etc.)

Language

The article should be in English. The grammar and style of the article should be of good quality. The systematized text should be without abbreviations (except standard ones). All measurements must be in SI units. The sequence of formulae is denoted in Arabic numerals in parentheses on the right-hand side.

Abstract and Summary

An abstract is a concise informative presentation of the article content for fast and accurate Evaluation of its relevance. It is both in the Editorial Office's and the author's best interest for an abstract to contain terms often used for indexing and article search. The abstract describes the purpose of the study and the methods, outlines the findings and state the conclusions. A 100- to 250-Word abstract should be placed between the title and the keywords with the body text to follow. Besides an abstract are advised to have a summary in English, at the end of the article, after the Reference list. The summary should be structured and long up to 1/10 of the article length (it is more extensive than the abstract).

Keywords

Keywords are terms or phrases showing adequately the article content for indexing and search purposes. They should be allocated heaving in mind widely accepted international sources (index, dictionary or thesaurus), such as the Web of Science keyword list for science in general. The higher their usage frequency is the better. Up to 10 keywords immediately follow the abstract and the summary, in respective languages.

Acknowledgements

The name and the number of the project or programmed within which the article was realized is given in a separate note at the bottom of the first page together with the name of the institution which financially supported the project or programmed.

Tables and Illustrations

All the captions should be in the original language as well as in English, together with the texts in illustrations if possible. Tables are typed in the same style as the text and are denoted by numerals at the top. Photographs and drawings, placed appropriately in the text, should be clear, precise and suitable for reproduction. Drawings should be created in Word or Corel.

Citation in the Text

Citation in the text must be uniform. When citing references in the text, use the reference number set in square brackets from the Reference list at the end of the article.

Footnotes

Footnotes are given at the bottom of the page with the text they refer to. They can contain less relevant details, additional explanations or used sources (e.g. scientific material, manuals). They cannot replace the cited literature.
The article should be accompanied with a cover letter with the information about the author(s): surname, middle initial, first name, and citizen personal number, rank, title, e-mail address, and affiliation address, home address including municipality, phone number in the office and at home (or a mobile phone number). The cover letter should state the type of the article and tell which illustrations are original and which are not.

Address of the Editorial Office:

Enriched Publications Pvt. Ltd.
S-9,IInd FLOOR, MLU POCKET,
MANISH ABHINAV PLAZA-II, ABOVE FEDERAL BANK,
PLOT NO-5, SECTOR -5, DWARKA, NEW DELHI, INDIA-110075,
PHONE: - + (91)-(11)-45525005

Notes: